

AD-A146 528

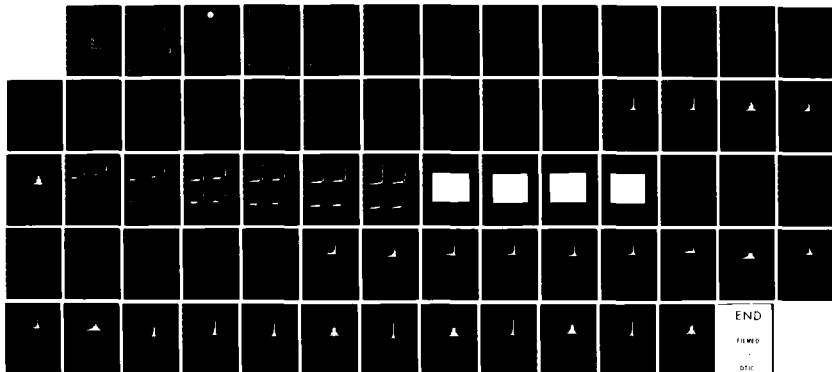
PRACTICAL APPLICATION OF IREPS (INTEGRATED REFRACTIVE
EFFECTS PREDICTION SYSTEM)(U) NAVAL OCEAN SYSTEMS
CENTER SAN DIEGO CA R A PAULUS 29 JUN 84 NOSC/TR-966

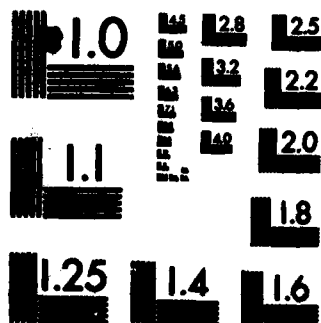
1/1

UNCLASSIFIED

F/G 4/2

NL





OPY RESOLUTION TEST CHART

12

NOSC TR 966

NOSC TR 966

Technical Report 966

PRACTICAL APPLICATION OF THE IREPS EVAPORATION DUCT MODEL

R. A. Paulus

29 June 1984
Interim Report

Prepared for
Naval Air Systems Command
Code 330

AD-A146 528

DTIC
ELECTE
OCT 15 1984
S D E

Approved for public release; distribution unlimited

DTIC FILE COPY

NOSC

NAVAL OCEAN SYSTEMS CENTER
San Diego, California 92152

84 10 11 005



NAVAL OCEAN SYSTEMS CENTER SAN DIEGO, CA 92152

AN ACTIVITY OF THE NAVAL MATERIAL COMMAND

J.M. PATTON, CAPT, USN

Commander

R.M. HILLYER

Technical Director

ADMINISTRATIVE INFORMATION

This task was performed for the Naval Air Systems Command, Code 330, Washington, DC 20362, under program element 62759N, subproject SF59551001.

Released by
H.V. Hitney, Head
Tropospheric Branch

Under authority of
Dr. J.H. Richter, Head
Ocean and Atmospheric
Sciences Division

RB

UNCLASSIFIED

SECURITY CLASSIFICATION OF THIS PAGE

REPORT DOCUMENTATION PAGE

1a. REPORT SECURITY CLASSIFICATION UNCLASSIFIED		1b. RESTRICTIVE MARKINGS	
2a. SECURITY CLASSIFICATION AUTHORITY		3. DISTRIBUTION/AVAILABILITY OF REPORT Approved for public release; distribution unlimited.	
2b. DECLASSIFICATION/DOWNGRADING SCHEDULE			
4. PERFORMING ORGANIZATION REPORT NUMBER NOSC Technical Report 966		5. MONITORING ORGANIZATION REPORT NUMBER N/A	
6a. NAME OF PERFORMING ORGANIZATION Naval Ocean Systems Center	6b. OFFICE SYMBOL (If applicable) Code 5430	7a. NAME OF MONITORING ORGANIZATION N/A	
6c. ADDRESS (City, State and ZIP Code) San Diego, CA 92152		7b. ADDRESS (City, State and ZIP Code) N/A	
8a. NAME OF FUNDING/SPONSORING ORGANIZATION Naval Air Systems Command	8b. OFFICE SYMBOL (If applicable) Code 330	9. PROCUREMENT INSTRUMENT IDENTIFICATION NUMBER	
8c. ADDRESS (City, State and ZIP Code) Washington, DC 20362		10. SOURCE OF FUNDING NUMBERS	
		PROGRAM ELEMENT NO. 62759N	PROJECT NO. SF59551001
		TASK NO. SF59551001	WORK UNIT NO. MP33
11. TITLE (Include Security Classification) PRACTICAL APPLICATION OF THE IREPS EVAPORATION DUCT MODEL			
12. PERSONAL AUTHOR(S) R. A. Paulus			
13a. TYPE OF REPORT Interim	13b. TIME COVERED FROM Oct 83 TO Apr 84	14. DATE OF REPORT (Year, Month, Day) 1984 June 29	15. PAGE COUNT 68
16. SUPPLEMENTARY NOTES			
17. COBAN CODES		18. SUBJECT TERMS (Continue on reverse if necessary and identify by block number)	
FIELD	GROUP	SUB-GROUP	Atmospheric Refraction of Electromagnetic Waves Evaporation Ducts IREPS
19. ABSTRACT (Continue on reverse if necessary and identify by block number)			
<p>The application of the IREPS evaporation duct model in operational and climatological propagation assessments and the sensitivity of the model to meteorological measurements are examined. The unexpectedly high occurrence of evaporation duct heights greater than 40 metres is related to stable conditions (positive air-sea temperature difference) in the surface layer. The existence of stable conditions over the ocean is analyzed in terms of meteorological conditions and temperature measurement accuracies. Comparisons of air-sea temperature difference distributions are made between high quality NOAA data buoy climatological data and archived ship surface weather data. A modification to the evaporation duct model is proposed and applied to radio-meteorological data.</p>			
20. DISTRIBUTION/AVAILABILITY OF ABSTRACT		21. ABSTRACT SECURITY CLASSIFICATION	Agency Accession
<input checked="" type="checkbox"/> UNCLASSIFIED/UNLIMITED <input type="checkbox"/> SAME AS RPT <input type="checkbox"/> DTIC USERS		Unclassified	DN888 715
22a. NAME OF RESPONSIBLE INDIVIDUAL R. A. Paulus		22b. TELEPHONE (Include Area Code) (619) 225-7247	22c. OFFICE SYMBOL Code 5325

assessing

copy

A

A

CONTENTS

INTRODUCTION . . . Page 1

OBSERVED PROBLEMS . . . 2

 OPERATIONAL ASSESSMENTS . . . 2

 CLIMATOLOGICAL ASSESSMENTS . . . 2

EVAPORATION DUCT PARAMETER MEASUREMENTS . . . 4

 ACCURACY . . . 4

 CLIMATOLOGICAL AIR-SEA TEMPERATURE DIFFERENCES . . . 4

SENSITIVITY OF THE IREPS EVAPORATION DUCT MODEL . . . 6

 METEOROLOGICAL RELATIONSHIPS WITH EVAPORATION DUCT HEIGHT . . . 6

 Unstable . . . 6

 Stable . . . 6

 MEASUREMENT ACCURACIES . . . 7

SUMMARY . . . 11

RECOMMENDATIONS . . . 12

REFERENCES . . . 41

APPENDIX A: HISTOGRAMS OF AIR-SEA TEMPERATURE DIFFERENCES . . . 43

Accession For	
NTIS GRA&I	<input checked="" type="checkbox"/>
DTIC TAB	<input type="checkbox"/>
Unannounced	<input type="checkbox"/>
Justification	
By _____	
Distribution/	
Availability Codes	
Dist	Avail and/or Special
A-1	



OBJECTIVES

Investigate the validity of high (30-40 metres) evaporation duct heights in operational assessments and climatologies of the evaporation duct. Establish the sensitivity of the IREPS evaporation duct model to the input parameters.

RESULTS

1. Air-sea temperature differences as measured by transiting ships are found to be biased toward thermally stable conditions when compared to high quality NOAA data buoy data.
2. The IREPS evaporation duct model is shown to be more sensitive to the relative accuracy of air-sea temperature difference than the absolute accuracy of the measured parameters.
3. The IREPS evaporation duct model can be modified to greatly diminish the occurrence of high duct heights resulting from biased air temperature measurements.

RECOMMENDATIONS

1. Adopt the modified evaporation duct model for use in IREPS.
2. Reanalyze the evaporation duct climatology with the modified evaporation duct model.
3. Develop a new sensor that would measure both air and sea temperature with high relative accuracy and be subject to a minimum of ship induced effects. A sensor with a resolution of 0.1°C and an absolute accuracy of 0.5°C is suggested.

INTRODUCTION

The Integrated Refractive Effects Prediction System (IREPS) has been used
utilized operationally by the U.S. Navy since 1978. Subsequently, there have
been questions from the fleet concerning IREPS assessments of system perform-
ance under strong (30-40 metres) evaporation ducting conditions that have not
been borne out by observed system performance. Additionally, the IREPS
climatological propagation assessments developed from the National Climatic
Data Center (NCDC) data base show a distinctly bimodal distribution of evapo-
ration duct heights that is difficult to justify. Errors in system perform-
ance assessment arise in three areas: (1) the environmental measurements, (2)
the meteorological models used to determine evaporation duct heights, and (3)
the propagation models used to quantify propagation conditions. Only the
first two of these areas are investigated in this report.

conting A

OBSERVED PROBLEMS

OPERATIONAL ASSESSMENTS

Assessment of system performance is done operationally with IREPS by entering current environmental data, both surface and upper air. Surface data required are wind speed, sea-surface temperature, air temperature, and relative humidity. Upper air data required are pressure, temperature, and relative humidity at levels of significant change. Upper air data establish the presence of surface-based ducts which will extend surface-to-surface propagation for all frequencies above 100 MHz. In the absence of any refractive effects from elevated layers, the evaporation duct is the dominant factor in surface-to-surface propagation, the strength of which is determined from surface meteorological measurements. The enhancement effect of the evaporation duct is highly frequency dependent, and variations in evaporation duct height will result in variations of assessed performance. Table 1 is an example of computed duct height for a 24-hour period for a CV in the southern California operating area. Weather was scattered to broken clouds, becoming clear after 1400, and winds were moderate northwesterly. Under these conditions, one would expect the evaporation duct to be fairly uniform with time, yet computed duct height varied from 10 to 40 metres. This is typical of those situations where actual system performance changes little even though assessed performance varies dramatically.

It is recognized that there are problems with observing the evaporation duct parameters at sea. Winds must be determined from the observed relative wind; air temperature and relative humidity are determined from dry- and wet-bulb psychrometric measurements which are subject to ship-induced effects; sea surface temperature is often taken from the seawater injection temperature, the inlet for which is well below the surface and is also subject to ship induced effects. Still, the evaporation duct height calculations are not unreasonable except in the cases where air temperature is greater than sea temperature and computed duct height goes to 30 to 40 metres. Stable conditions and relative humidities in the range of 65-75% would not be expected in the open ocean. This indicates that errors in air-sea temperature difference, to which the evaporation duct height calculation can be quite sensitive, may be the contributing factor in unrealistically high evaporation duct heights.

CLIMATOLOGICAL ASSESSMENTS

The IREPS evaporation duct height climatology was compiled from NCDC archived ship surface weather observations for the years 1970 to 1979 and reported in reference 1. This climatology has been incorporated into the IREPS historical data base and has been published as part of reference 2. Figure 1 shows representative duct height distributions for the open ocean areas around and north of Hawaii. Notice that all distributions are bimodal and that the percent occurrence of duct heights of 40 metres or greater varies diurnally and latitudinally. Evaporation duct heights of 40 metres would effectively enhance propagation for frequencies as low as 1 GHz. Results from propagation experiments such as reference 3 do not support the relatively high percent occurrence of ducting as indicated by climatology. The diurnal and latitudinal variation of the occurrence of 40-metre ducts implicates solar insolation in possible air-sea temperature difference measurement errors. It is very likely that the erroneously measured stable conditions discussed in the previous section have biased the evaporation duct climatology.

Table 1. Hourly evaporation duct heights calculated from surface weather observations taken on board a carrier operating 350 nmi southwest of San Diego on 10 October 1983.

Time(local)	Wind(kts)	Ts(C)	Ta(C)	RH(%)	Delta(m)
0000	14	21.3	20.9	88	10.1
0100	8	21.3	20.6	78	12.6
0200	10	21.3	20.8	74	16.6
0300	11	21.3	20.7	72	17.7
0400	10	21.3	20.7	72	16.7
0500	14	21.1	20.4	76	16.6
0600	18	21.1	20.2	75	18.7
0700	19	21.1	20.8	77	18.3
0800	14	23.3	21.7	76	17.8
0900	18	23.3	22.8	73	22.2
1000	17	23.3	22.9	68	26.5
1100	19	23.3	23.1	72	24.4
1200	18	23.3	21.1	76	18.7
1300	14	23.3	21.8	75	17.6
1400	17	22.2	22.2	76	21.8
1500	20	22.2	22.8	76	23.8
1600	24	22.2	22.8	66	34.1
1700	20	22.2	23.8	72	28.5
1800	18	22.2	22.9	65	48.8
1900	20	22.2	21.4	64	26.5
2000	21	22.2	21.6	76	19.7
2100	24	22.2	20.9	82	16.4
2200	24	22.2	21.4	88	17.9
2300	18	23.3	20.7	84	15.4

EVAPORATION DUCT PARAMETER MEASUREMENTS

ACCURACY

The elements of wind speed, air and sea-surface temperature, and relative humidity as measured by transiting ships have, in the past, been sufficiently accurate for operational and general climatological purposes. Reference 4 indicates that air temperature is generally reliable, but notes that temperatures reported by ships in the tropics appear to be consistently high under sunny conditions due to poor instrument exposure. Sea-surface temperatures are somewhat less reliable due to varied observational methods. Reference 5 reports average errors on the order of $+1^{\circ}\text{C}$ for seawater injection temperatures versus bucket temperatures. Surface temperatures obtained from expendable bathythermographs are potentially the most accurate routine sea-surface temperatures currently made, but most U.S. Navy ships eject the instrument into the ship's wake. On the whole, the absolute accuracy of the measurements of the evaporation duct parameters is adequate; however, the relative accuracy of the air and sea temperatures has the greatest impact on evaporation duct height determination. These two elements are usually obtained by different instruments and different observers, compounding the problem.

CLIMATOLOGICAL AIR-SEA TEMPERATURE DIFFERENCES

The National Oceanic and Atmospheric Administration (NOAA) has incorporated marine data buoys in the NCDC data base and published summaries (reference 6). The buoy data include wind speed and air and sea temperature observations and represent data superior to that available from ship observations as specific actions were taken in buoy design to avoid platform induced effects. Unfortunately, moisture data are not available, so evaporation duct calculations cannot be made. However, air-sea temperature differences and bulk Richardson's numbers can be examined. Buoy locations are shown in figure 2. Most of the buoys in the Atlantic and the Gulf of Mexico are subject to continental influences which will tend to increase the extremes of air-sea temperature difference distributions. However, these data should bound the open ocean conditions. Pacific buoy data should be representative of the open ocean. Buoys in both ocean regions can be compared to archived ship data within those regions to determine the extent to which the IREPS climatology is biased.

It has already been noted that air temperature observations from ships in the tropics tend to be consistently high on sunny days. NOAA data buoys 42001 and 42002 are located in Marsden square 82 and 42003 in Marsden square 81 (the evaporation duct climatology in IREPS is geographically organized by Marsden square). The air-sea temperature difference (ASTD) distributions derived from reference 6 are shown in figure 3, as are the distributions from the IREPS historical data base for these two Marsden squares. Buoys 42001 and 42002 indicated stable conditions (ASTD>0) 7.3% and 1.3% of the time, respectively, compared to 34.8% of the time for the IREPS historical; buoy 42003 indicates stable conditions 0.7% of the time compared to 30.8% of the time for IREPS. Even allowing for point observations versus observations over the entire Marsden square, the discrepancy between the buoy data and ship data strongly indicates a bias in the ship data. The result of the bias is that the IREPS historical data indicate evaporation duct heights of 40 metres or greater more than 15% of the time annually in these two Marsden squares. The remaining

buoy and Marsden square data are in appendix A and further confirm the ASTD discrepancies.

Another feature of the IREPS historical data base is that it is broken down into day and night distributions. This was done to examine any diurnal variations; however, the variation that does show up is stronger than expected. Table 2, derived from reference 7, shows diurnal temperature variations at several buoys to be less than 0.6°C, implying a much smaller diurnal variation in evaporation duct height than is currently analyzed. Table 2 also belies the diurnal variation reported by ships and further supports the likelihood of a bias toward stable conditions.

Table 2. Diurnal variation of temperature at five NOAA data buoys from the mean air temperature at 3-hour intervals; Greenwich Mean Time (GMT) and Local Standard Time (LST).

BUOY	GMT	00	03	06	09	12	15	18	21	ALL HRS
	LST	19	22	01	04	07	10	13	16	
41001	35.0N 72.0W	19.54	19.56	19.37	19.30	19.37	19.51	19.58	19.66	19.49
41005	31.7N 79.7W	21.07	21.90	21.05	21.73	21.47	21.56	21.56	21.02	21.73
44003	40.0N 60.5W	9.74	9.74	9.67	9.51	9.60	9.76	9.91	9.93	9.73
	LST	10	21	00	03	06	09	12	15	
42001	26.0N 90.0W	24.76	24.59	24.53	24.40	24.41	24.79	24.94	24.98	24.67
	LST	14	17	20	23	02	05	08	11	
46001	56.0N 140.0W	5.00	5.73	5.62	5.60	5.55	5.51	5.63	5.01	5.66

SENSITIVITY OF THE IREPS EVAPORATION DUCT MODEL

The evaporation duct model used in IREPS is basically the model developed by Jeske (reference 8) and adapted by Hitney (reference 9). Figure 4 shows the variation of duct height versus air-sea temperature difference parametrically in relative humidity for various sea temperatures and wind speeds commonly encountered in the open ocean. As discussed by Anderson (reference 10), the curves are well-behaved for thermally unstable conditions but vary dramatically under stable conditions. Lower relative humidity and lower wind speed also affect the curves for even slightly unstable conditions. Even small errors in measuring air-sea temperature difference can lead to large errors in evaporation duct height on the stable side of the diagrams.

METEOROLOGICAL RELATIONSHIPS WITH EVAPORATION DUCT HEIGHT

Over the open ocean, air-sea temperature differences are normally slightly negative. In the presence of large ocean currents, in regions of upwelling, and with the movement of warm or cool air masses, contrasts of ASTD are greater. Under continental influences, the contrasts are greater still. The ASTD distributions for the NOAA data buoys in appendix A substantiate this. The relationships between meteorological conditions and the resulting evaporation ducting conditions give insight to the practical application of the evaporation duct model.

Unstable

In the absence of advective effects, the marine surface layer is typically slightly unstable due to the different heat capacities of air and water. Cool air being advected over warmer water will create even greater instability; cold continental air flowing out over the ocean will create the strongest instability. However, figure 4 shows the evaporation duct height to be relatively insensitive to increasingly negative air-sea temperature differences and thus also to errors in measuring the difference.

Stable

Stable conditions over the open ocean would not be expected in the absence of advection. Figure 4 indicates two possible situations with diverse evaporation duct heights associated with each situation. The first situation is one in which warm, high-humidity air overlies cooler water. This would occur with advection across an ocean current toward the cool side, advection toward an upwelling region, or with warm frontal passage. In figure 4, this is the situation in which evaporation duct height continually decreases with increasing air-sea temperature difference. This is because the refractivity difference between the surface and the observation height is continually decreasing. This type of meteorological situation is also conducive to fog formation as the overlying air is cooled by air-sea interaction and its relative humidity increases to the point of condensation. It is speculated that the higher percent occurrence of stable conditions at buoys 44001-5 shown in appendix A is due to this type of situation. The region in which these buoys are located does have a high incidence of low visibilities. This theory rectifies, in part, the fact that the percent occurrence of stable conditions is far greater than the percent occurrence of 40-metre evaporation ducts. This same argument holds for buoy 46006 in the Pacific as well.

The second stable situation is one in which warm, lower-humidity air overlies cooler water. This would have to occur in ocean areas under a continental influence. Santa Anas in the southern California area are one of this type of influence. Extremely high evaporation duct heights would result, as shown by the lower relative humidity lines in figure 4 that initially increase with air-sea temperature difference and then eventually decrease. The maximum on the curves is the point where δ/L' becomes greater than one and duct height is recomputed based upon the limit $\delta/L' = 1$ (references 8, 9). Duct height then decreases toward zero as the refractivity differences decrease. Evaporation duct heights of 40 metres or greater are common in this situation and system performance assessment would indicate strong enhancements. However, it is argued that, in this situation, surface-to-surface propagation would be dominated by a larger surface-based duct that would likely be associated with the temperature inversion at the top of the boundary layer. Thus, the evaporation duct is of little relative importance in this case.

MEASUREMENT ACCURACIES

Since the meteorological situation of relatively warm air and low humidity should not exist over the ocean without other propagation mechanisms being dominant, it is possible to modify the evaporation duct calculation to prevent measurement inaccuracies from falsely indicating this type of meteorological situation and the resulting high and unrealistic duct heights. From figure 4 it can be seen that there is only a small error in determining duct height from fairly large errors in air-sea temperature difference as long as air-sea temperature difference is less than approximately -5°C . For air-sea temperature differences greater than -5°C , errors in duct height will increase and, in particular, can be quite large for even small errors in air-sea temperature difference for relative humidities less than 90%. It is then desirable to determine a maximum air-sea temperature difference above which increasing duct heights would be neglected but decreasing duct heights would be allowed. Table 3 shows mean air-sea temperature differences for the NOAA data buoys. Table 4 shows air-sea temperature differences for a variety of temperatures and wind speeds at which the bulk Richardson's number (reference 9) is -0.03 ($|Ri_b| \leq 0.03$ are considered to be near-neutral conditions). These data suggest a maximum air-sea temperature difference between 0 and -1°C would be reasonable. To see the effect that an air-sea temperature difference limit would have, data collected by Anderson (reference 3) in June 1982 were reanalyzed. Figure 5a is a plot of observed pathloss at 17.7 GHz versus calculated duct height. The red data points are those duct heights computed from meteorological data that indicated stable conditions ($\text{ASTD} > 0$). Although this plot is scaled to only 25 metres, red data points occurred up to and beyond 40 metres. The yellow, green, and blue data points are those with ASTD values as indicated in the figure. The solid lines are theoretical curves calculated by waveguide techniques for a smooth sea surface and three stability conditions. Notice that the blue points are in closest agreement with the theoretical curves, whereas the red points tend to indicate far greater pathloss than predicted for the duct height. This strongly indicates erroneous temperature measurements since the errors tend to increase with air-sea temperature difference. If this is the case, these data would show a marked improvement in correlation using a modified evaporation duct height calculation, and the best correlation would be indicative of an ASTD threshold above which all data would be subject to the modification technique. Figures

Table 3. Monthly and annual mean air-sea temperature differences for NOAA data buoys (reference 6).

BUOY	LOCATION	JAN	FEB	MAR	APR	MAY	JUN	JUL	AUG	SEP	OCT	NOV	DEC	ANN
41001	39.0N 72.0W	-6.2	-6.2	-3.7	-2.5	-0.0	-0.4	-0.4	-0.7	-1.2	-2.9	-4.5	-5.4	-3.0
41002	32.3N 75.2W	-6.2	-4.9	-3.9	-2.3	-1.3	-0.9	-0.0	-1.4	-1.6	-2.0	-3.3	-5.2	-2.7
41004	32.6N 70.7W	-6.2	-5.0	-1.0	-1.1	-0.5	-0.7	-0.6	-0.0	-1.2	-2.0	-4.5	-6.3	-2.4
41005	31.7N 79.7W	-6.3	-5.4	-3.1	-0.5	-0.9	-0.6	-0.4	-0.7	-1.3	-3.0	-4.5	-6.1	-2.5
42001	25.0N 90.0W	-3.5	-2.6	-0.0	-0.5	-0.5	-0.0	-0.6	-0.7	-0.0	-1.1	-1.4	-2.2	-1.2
42002	25.0N 93.5W	-2.0	-2.2	-1.0	-0.5	-0.4	-0.6	-0.9	-1.2	-1.2	-2.0	-2.4	-2.2	-1.5
42003	26.0N 06.0W	-4.4	-4.4	-2.0	-1.0	-1.2	-0.8	-1.1	-1.1	-1.1	-2.0	-3.3	-4.3	-2.3
44001	30.7N 73.6W	-5.1	-3.1	-0.1	.5	1.1	.6	-0.1	-0.3	-0.6	-1.1	-1.7	-4.6	-1.5
44002	40.1N 73.0W	-5.6	-4.0	-0.4	.9	1.1	.6	.1	-0.1	-0.6	-1.7	-2.3	-4.7	-1.1
44003	40.0N 60.5W	-4.4	-2.7	-0.4	.0	1.5	2.1	2.7	2.1	.7	-1.1	-2.1	-3.7	-0.2
44004	39.0N 70.0W	-7.2	-6.6	-5.5	-1.1	-0.4	-0.8	-1.0	-1.1	-2.1	-4.4	-5.8	-6.9	-4.0
44005	42.7N 60.5W	-6.7	-6.7	-2.1	-0.2	.5	.5	.7	-0.4	-0.1	-1.4	-1.0	-5.0	-1.9
46001	56.0N 140.0W	-0.6	-1.1	-0.0	-0.7	-0.5	-0.3	-0.4	-0.3	-0.6	-1.1	-1.5	-2.5	-1.0
46002	42.5N 130.0W	-1.5	-1.0	-1.5	-1.0	-1.5	-1.5	-1.3	-1.2	-1.3	-1.6	-1.8	-1.2	-1.4
46003	52.0N 150.0W	-0.0	-1.0	-0.5	-0.4	-0.4	-0.1	-0.3	-0.3	-0.0	-1.4	-1.0	-1.0	-0.9
46004	51.0N 136.0W	-0.2	-0.4	-0.2	-0.3	-0.2	-0.1	-0.0	-0.3	-0.3	-0.4	-0.7	-1.0	-0.4
46005	46.0N 131.0W	-0.4	-0.7	-0.7	-0.6	-0.6	-0.6	-0.5	-0.5	-0.6	-1.0	-1.3	-1.4	-0.9
46006	41.0N 130.0W	-3.7	-1.0	-0.6	-1.1	-0.3	.5	-0.3	.2	-0.4	-0.3	-0.9	-0.7	-0.5

Table 4. Air-sea temperature differences at which the bulk Richardson's number is -0.03 at selected temperature and wind speed combinations.

Sea Temp = 30C	Wind = 5 knots	Rib = -.03	ASTD = -.10C
Sea Temp = 30C	Wind = 10 knots	Rib = -.03	ASTD = -.41C
Sea Temp = 30C	Wind = 15 knots	Rib = -.03	ASTD = -.92C
Sea Temp = 30C	Wind = 20 knots	Rib = -.03	ASTD = -1.63C
Sea Temp = 30C	Wind = 25 knots	Rib = -.03	ASTD = -2.55C
Sea Temp = 25C	Wind = 5 knots	Rib = -.03	ASTD = -.10C
Sea Temp = 25C	Wind = 10 knots	Rib = -.03	ASTD = -.40C
Sea Temp = 25C	Wind = 15 knots	Rib = -.03	ASTD = -.91C
Sea Temp = 25C	Wind = 20 knots	Rib = -.03	ASTD = -1.61C
Sea Temp = 25C	Wind = 25 knots	Rib = -.03	ASTD = -2.50C
Sea Temp = 20C	Wind = 5 knots	Rib = -.03	ASTD = -.10C
Sea Temp = 20C	Wind = 10 knots	Rib = -.03	ASTD = -.40C
Sea Temp = 20C	Wind = 15 knots	Rib = -.03	ASTD = -.89C
Sea Temp = 20C	Wind = 20 knots	Rib = -.03	ASTD = -1.58C
Sea Temp = 20C	Wind = 25 knots	Rib = -.03	ASTD = -2.46C
Sea Temp = 15C	Wind = 5 knots	Rib = -.03	ASTD = -.10C
Sea Temp = 15C	Wind = 10 knots	Rib = -.03	ASTD = -.39C
Sea Temp = 15C	Wind = 15 knots	Rib = -.03	ASTD = -.88C
Sea Temp = 15C	Wind = 20 knots	Rib = -.03	ASTD = -1.55C
Sea Temp = 15C	Wind = 25 knots	Rib = -.03	ASTD = -2.42C
Sea Temp = 10C	Wind = 5 knots	Rib = -.03	ASTD = -.10C
Sea Temp = 10C	Wind = 10 knots	Rib = -.03	ASTD = -.38C
Sea Temp = 10C	Wind = 15 knots	Rib = -.03	ASTD = -.86C
Sea Temp = 10C	Wind = 20 knots	Rib = -.03	ASTD = -1.53C
Sea Temp = 10C	Wind = 25 knots	Rib = -.03	ASTD = -2.38C
Sea Temp = 5C	Wind = 5 knots	Rib = -.03	ASTD = -.09C
Sea Temp = 5C	Wind = 10 knots	Rib = -.03	ASTD = -.38C
Sea Temp = 5C	Wind = 15 knots	Rib = -.03	ASTD = -.85C
Sea Temp = 5C	Wind = 20 knots	Rib = -.03	ASTD = -1.50C
Sea Temp = 5C	Wind = 25 knots	Rib = -.03	ASTD = -2.34C

|Rib| ≤ 0.03 ⇒ "near neutral"

5b, c, and d show the results of using a modified evaporation duct height calculation with thresholds of 0, -0.5, and -1°C ASTD, respectively. The yellow data points are those for which the ASTD threshold was exceeded and which were subjected to the modified technique; the blue data points are unchanged from the original data. In figure 5b, there are only a few data points above 15 metres and these are original data at lower pathloss values. The points plotted in yellow using the modified duct height calculation show improvement over figure 5a but still have considerable scatter as compared to the theoretical curves. Figures 5c and d show additional improvement, with figure 5d showing comparable scatter between the blue and yellow points; the higher duct heights (12-16m) now correspond to the lower pathloss values. This indicates a threshold of -1°C ASTD in the modified evaporation duct height calculation gives good agreement with these radio data.

To determine the possible effects that the modified evaporation duct height calculation would have on the IREPS climatology, a comparison of histograms is useful. Figure 6a shows the duct height distribution for Marsden square 120 for June from the IREPS climatology. Note the trimodal appearance of the daytime distribution with relative maximums at 0 to 2, 10 to 12, and greater than 40 metres. The lower and higher modes likely result from the large, positive air-sea temperature differences in the archived ship weather observations. Figure 6b shows the distribution of the (unmodified) data of figure 5a. This distribution is bimodal, shows a lower occurrence of daytime ducts greater than 40 metres, and has a greater kurtosis. Finally, figure 6c shows the distribution of the modified duct height data of figure 5d. This distribution is closer to a normal distribution; the bimodal characteristic is gone and kurtosis has increased further. The mean duct height shows only a slight diurnal variation and is lower than the means in figures 6a and b. This distribution is typical of what one would expect from geophysical data. It is anticipated that applying the modified evaporation duct height calculation to the archived ship surface meteorological data would have the effect of lowering the mean duct height and reducing the variance of duct height.

The modification to the evaporation duct height calculation is flow-charted in figure 7. If ASTD is less than or equal to -1, then the evaporation duct height, δ , is calculated using the ambient ASTD. Otherwise, δ is computed for both ASTD = -1 and ASTD = 0. If δ (ASTD = -1) is less than δ (ASTD = 0), then δ is set equal to the δ calculated with ASTD = -1. Otherwise, δ is calculated using ambient ASTD.

SUMMARY

Operational determinations of the evaporation duct and the IREPS historical data base show an unexpectedly high occurrence of evaporation duct heights of 40 metres or greater. These high duct heights occur under thermally stable conditions and lower relative humidities. These conditions are the result of (1) a continental influence or (2) temperature measurement errors. In the first case, a surface-based duct will also exist, dominate any evaporation duct effects, and produce propagation enhancements for all frequencies above 100 MHz. In the second case, propagation enhancement for all frequencies above 1 GHz will be falsely assessed. If the evaporation duct height is recomputed for stable conditions and lower relative humidities, assuming an air-sea temperature difference of -1 , system performance assessment in the first case will be unchanged (since the assessment would be based on surface-based duct effects) and system performance assessment in the second case will be based on data more likely to be representative of actual conditions. This modification of the evaporation duct calculation works well on propagation data obtained from an 18-GHz propagation link and indicates that the current IREPS duct height climatology is biased toward higher means and larger variances.

RECOMMENDATIONS

Based on this study, it is recommended that:

1. The evaporation duct calculation used by IREPS be modified as proposed to limit the occurrence of high duct heights.
2. The IREPS historical data base be updated by reanalyzing the NCDC data base using the modified evaporation duct height calculation.
3. A new sensor be developed that would be capable of measuring air and sea temperature to a high relative accuracy and would minimize ship induced effects. A sensor resolution of 0.1°C and absolute accuracy of 0.5°C is suggested.

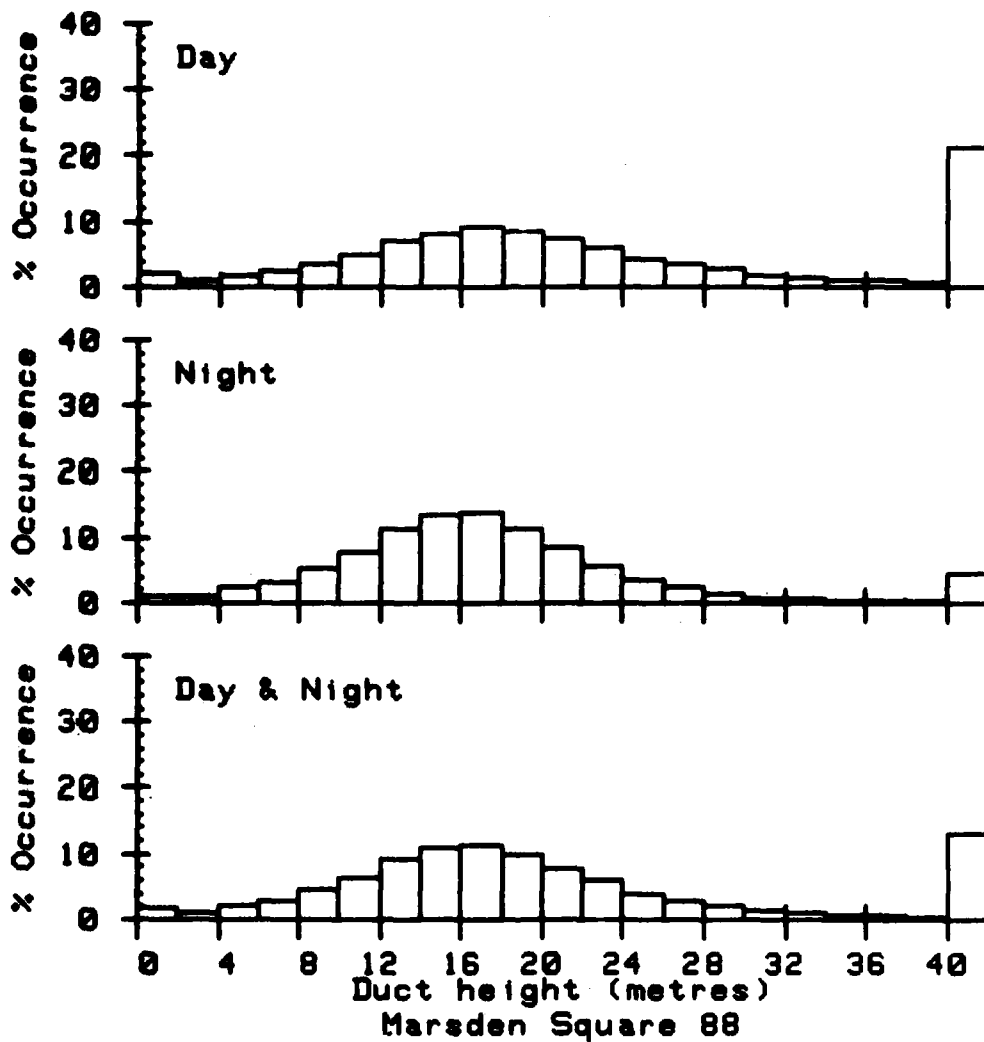


Figure 1a. Distribution of annual evaporation duct heights from the IREPS historical data base for Marsden square 88 centered at 25N 155W.

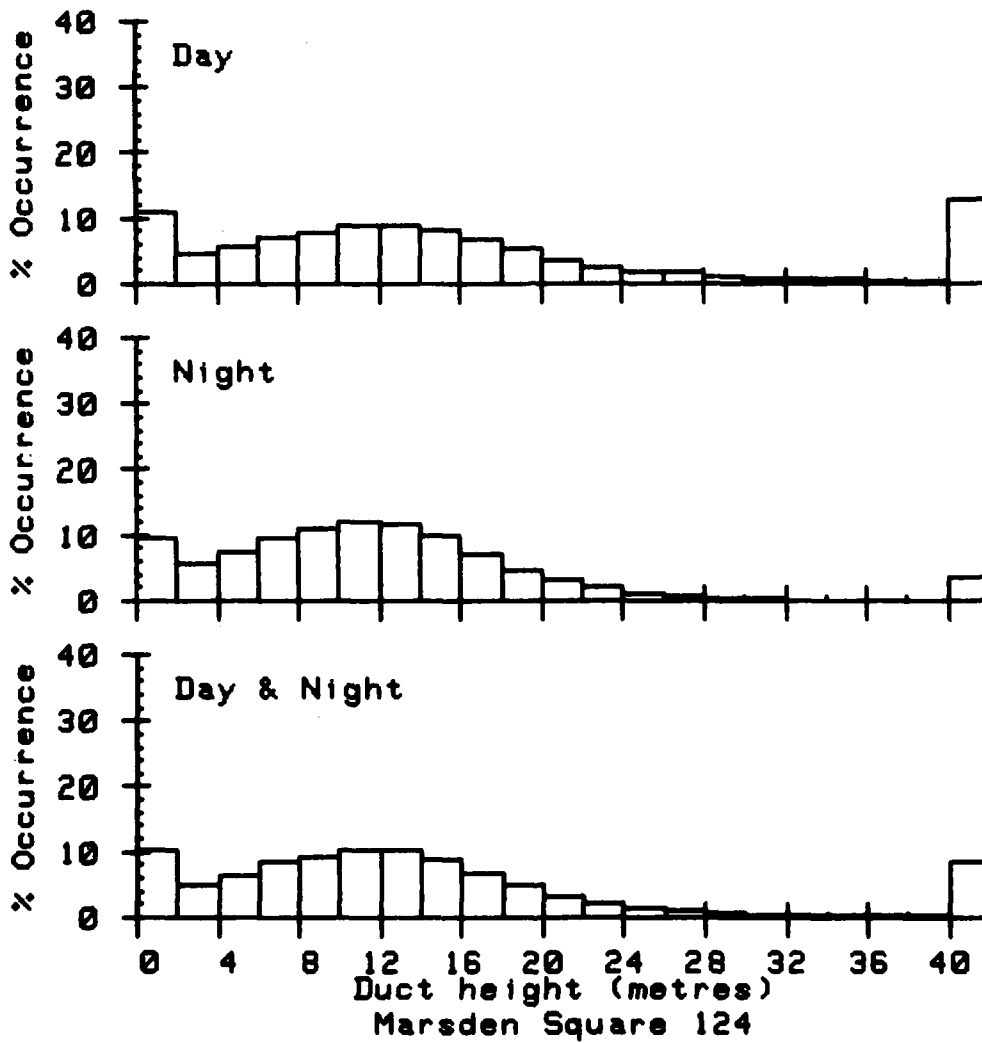


Figure 1b. Distribution of annual evaporation duct heights from the IREPS historical data base for Marsden square 124 centered at 35N 155W.

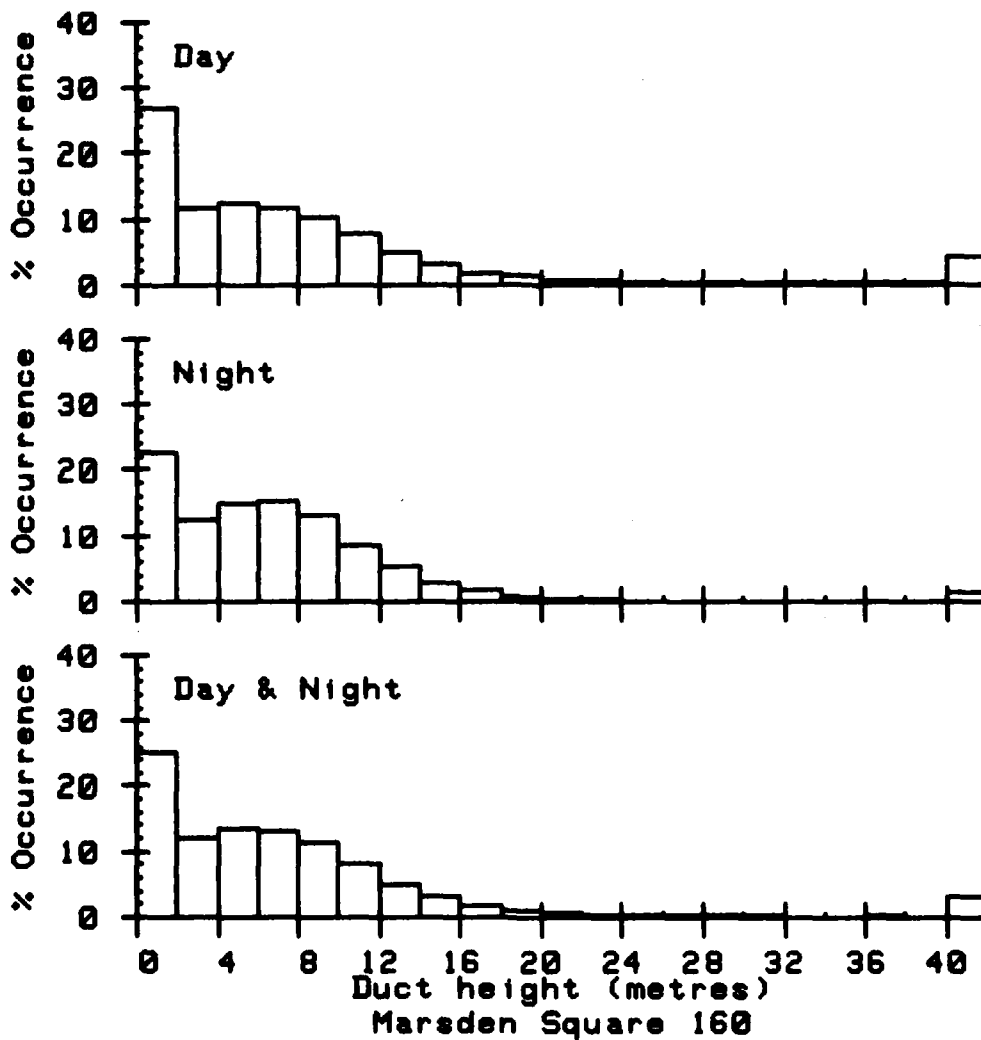


Figure 1c. Distribution of annual evaporation duct heights from the IREPS historical data base for Marsden square 160 centered at 45N 155W.

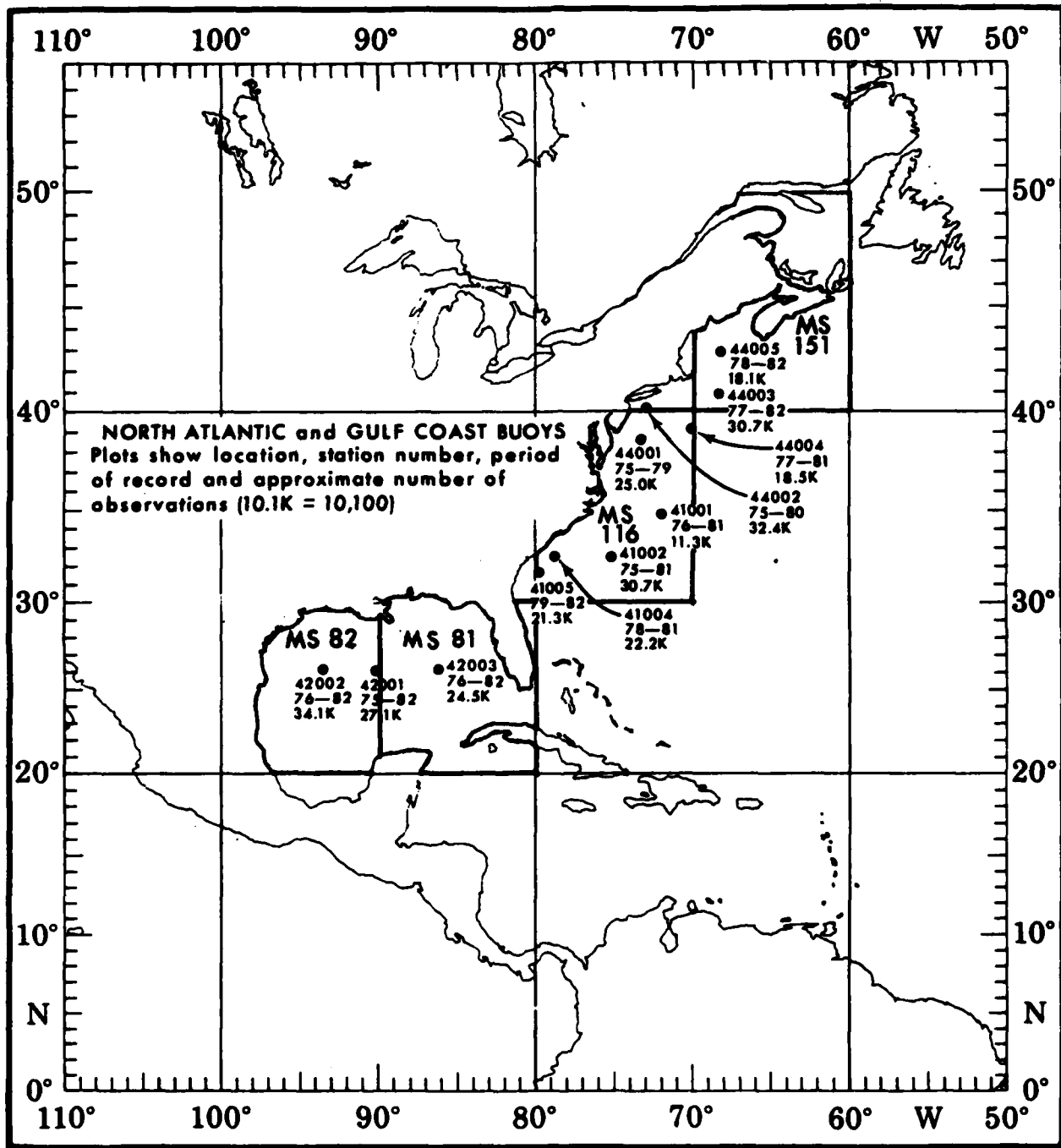


Figure 2a. North Atlantic and Gulf of Mexico buoys (from reference 6).

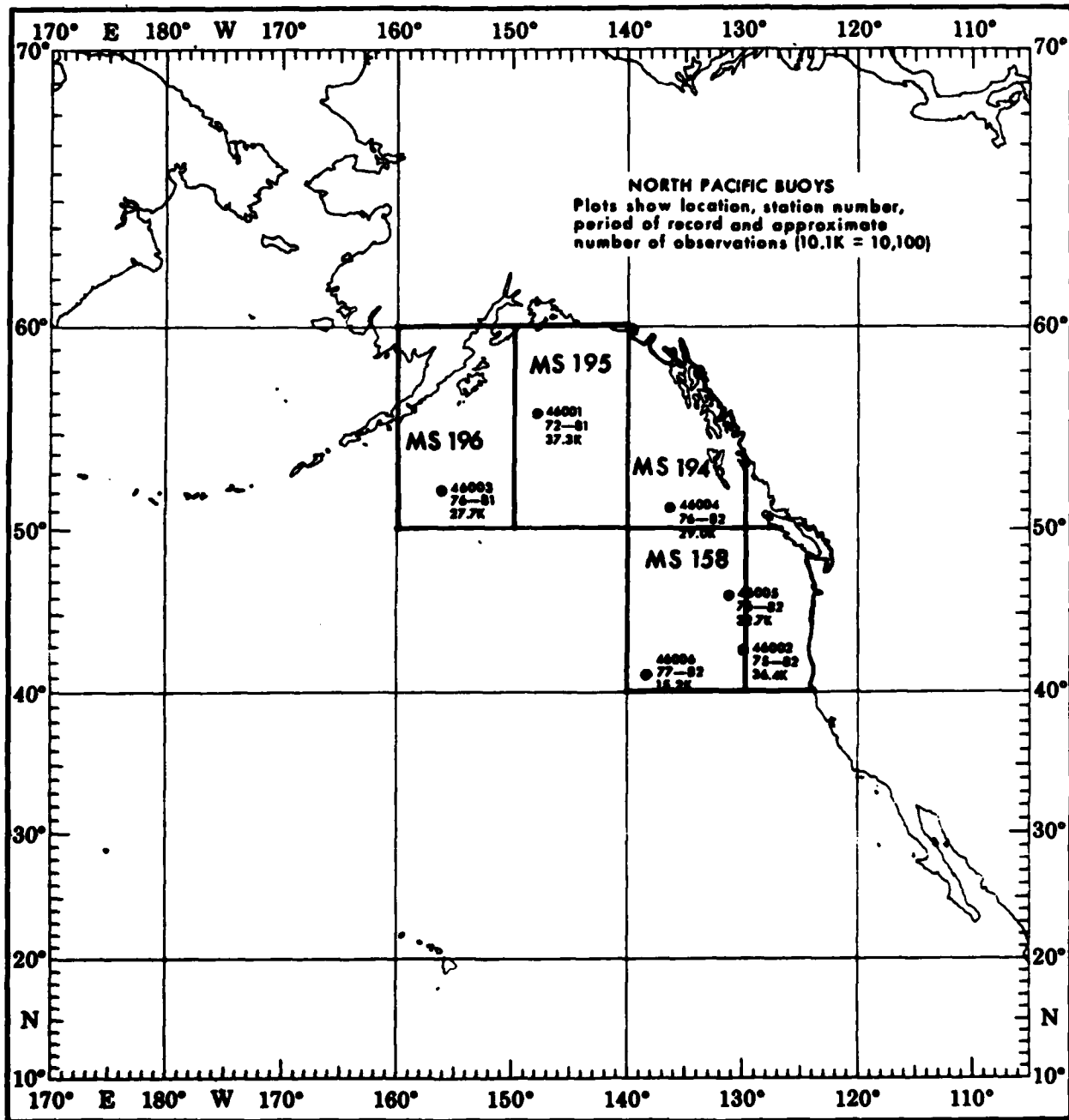
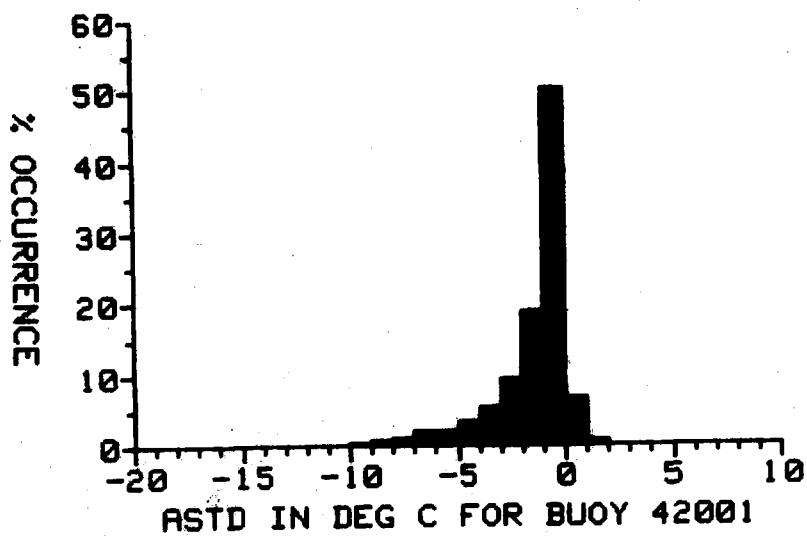


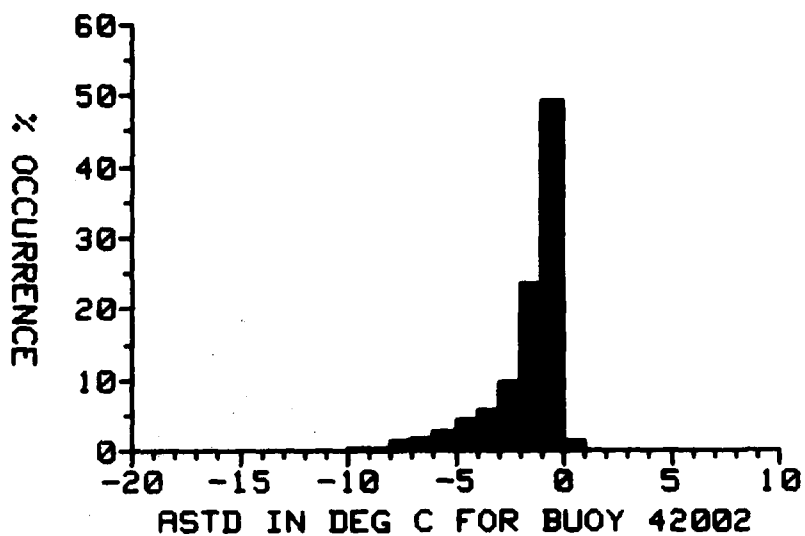
Figure 2b. North Pacific buoys (from reference 6).



-13<#	obs<=-12	2	.01%
-12<#	obs<=-11	7	.03%
-11<#	obs<=-10	5	.02%
-10<#	obs<= -9	52	.19%
-9<#	obs<= -8	155	.57%
-8<#	obs<= -7	288	1.06%
-7<#	obs<= -6	517	1.91%
-6<#	obs<= -5	515	1.90%
-5<#	obs<= -4	935	3.45%
-4<#	obs<= -3	1425	5.25%
-3<#	obs<= -2	2547	9.39%
-2<#	obs<= -1	5100	18.80%
-1<#	obs<= 0	13607	50.15%
0<#	obs<= 1	1805	6.65%
1<#	obs<= 2	158	.58%
2<#	obs<= 3	13	.05%

Total obs = 27131

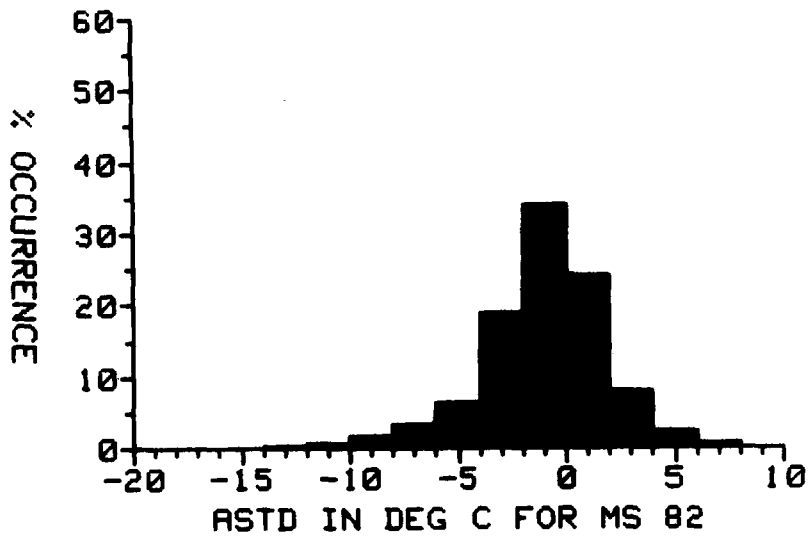
Figure 3a. Annual air-sea temperature difference distribution for buoy 42001 (from reference 6).



-15<#	obs<=-14	3	.01%
-14<#	obs<=-13	11	.03%
-13<#	obs<=-12	9	.03%
-12<#	obs<=-11	37	.11%
-11<#	obs<=-10	38	.11%
-10<#	obs<=-9	119	.35%
-9<#	obs<=-8	130	.38%
-8<#	obs<=-7	444	1.30%
-7<#	obs<=-6	576	1.69%
-6<#	obs<=-5	927	2.72%
-5<#	obs<=-4	1442	4.23%
-4<#	obs<=-3	1944	5.71%
-3<#	obs<=-2	3211	9.43%
-2<#	obs<=-1	7986	23.45%
-1<#	obs<= 0	16730	49.12%
0<#	obs<= 1	444	1.30%
1<#	obs<= 2	7	.02%
2<#	obs<= 3	1	.00%

Total obs = 34059

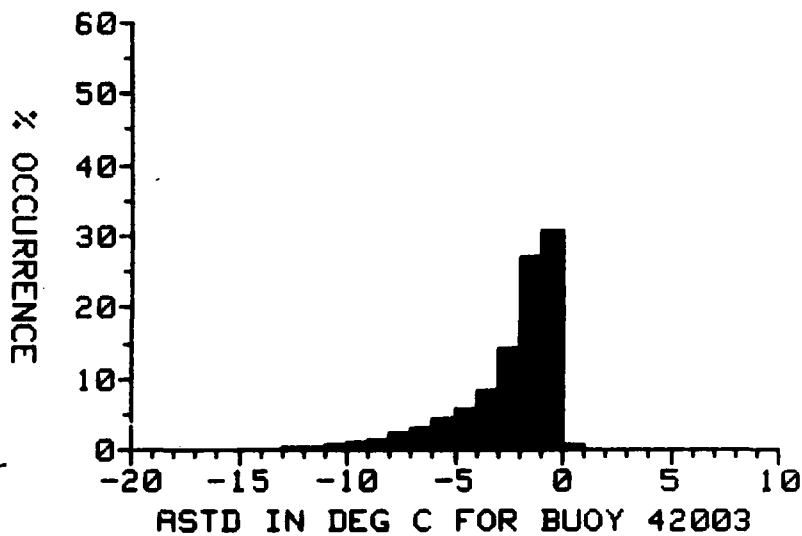
Figure 3b. Annual air-sea temperature difference distribution for buoy 42002 (from reference 6).



-18<#	obs<=-16	13	.03%
-16<#	obs<=-14	30	.07%
-14<#	obs<=-12	121	.28%
-12<#	obs<=-10	317	.73%
-10<#	obs<=-8	650	1.50%
-8<#	obs<=-6	1435	3.31%
-6<#	obs<=-4	2758	6.36%
-4<#	obs<=-2	8191	18.89%
-2<#	obs<= 0	14744	34.00%
0<#	obs<= 2	10368	23.91%
2<#	obs<= 4	3439	7.93%
4<#	obs<= 6	937	2.16%
6<#	obs<= 8	256	.59%
8<#	obs<= 10	65	.15%
10<#	obs<= 12	26	.06%
12<#	obs<= 14	9	.02%
14<#	obs<= 16	4	.01%
16<#	obs<= 18	4	.01%

Total obs = 43367

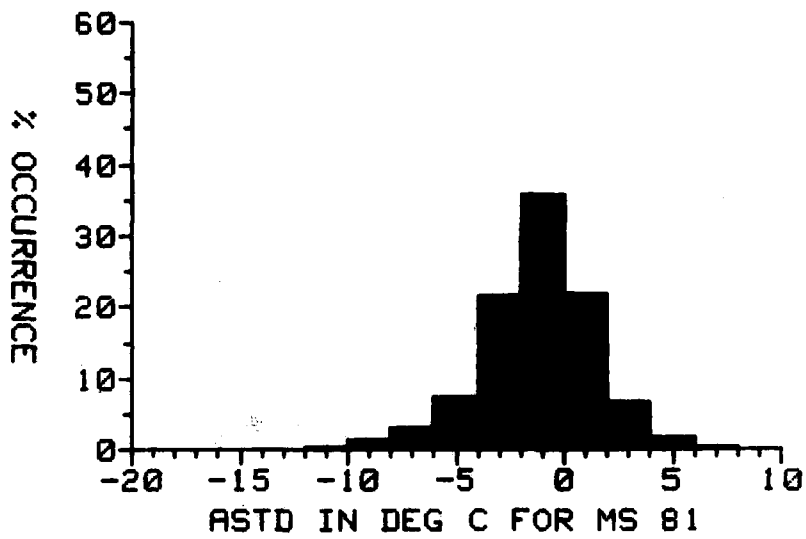
Figure 3c. Annual air-sea temperature difference distribution for Maraden square 82 (from reference 1).



-15<# obs<=-14	2	.01%
-14<# obs<=-13	23	.09%
-13<# obs<=-12	57	.23%
-12<# obs<=-11	114	.47%
-11<# obs<=-10	158	.64%
-10<# obs<=-9	267	1.09%
-9<# obs<=-8	362	1.48%
-8<# obs<=-7	561	2.29%
-7<# obs<=-6	714	2.91%
-6<# obs<=-5	1048	4.28%
-5<# obs<=-4	1386	5.65%
-4<# obs<=-3	2018	8.23%
-3<# obs<=-2	3447	14.06%
-2<# obs<=-1	6655	27.15%
-1<# obs<= 0	7521	30.69%
0<# obs<= 1	155	.63%
1<# obs<= 2	15	.06%
2<# obs<= 3	6	.02%
3<# obs<= 4	1	.00%

Total obs = 24518

Figure 3d. Annual air-sea temperature difference distribution for buoy 42003 (from reference 6).



-18<#	obs<=-16	30	.02%
-16<#	obs<=-14	60	.04%
-14<#	obs<=-12	238	.16%
-12<#	obs<=-10	596	.40%
-10<#	obs<=-8	1802	1.21%
-8<#	obs<=-6	4394	2.95%
-6<#	obs<=-4	10664	7.16%
-4<#	obs<=-2	32111	21.56%
-2<#	obs<= 0	53082	35.64%
0<#	obs<= 2	32439	21.78%
2<#	obs<= 4	9949	6.68%
4<#	obs<= 6	2681	1.80%
6<#	obs<= 8	670	.45%
8<#	obs<= 10	164	.11%
10<#	obs<= 12	45	.03%

Total obs = 148925

Figure 3e. Annual air-sea temperature difference distribution for Marsden square 81 (from reference 1).

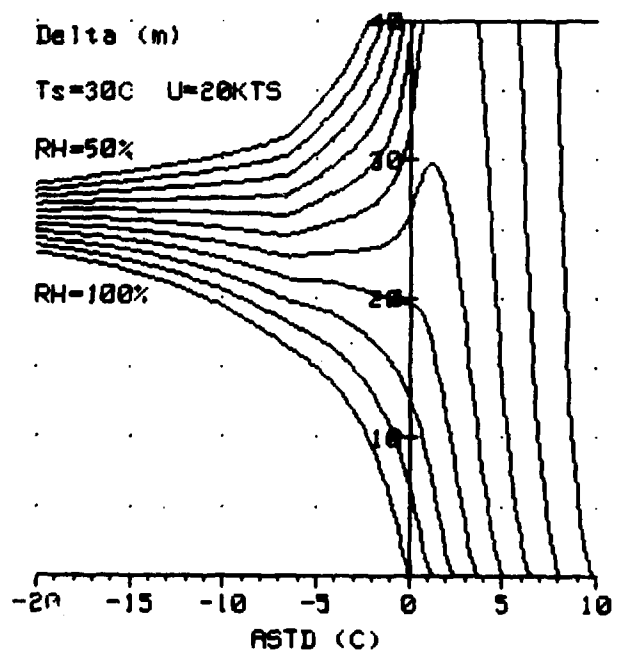
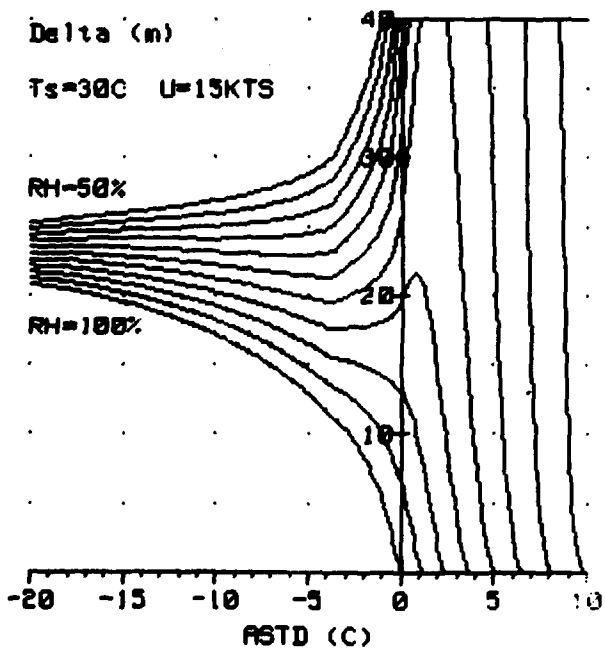
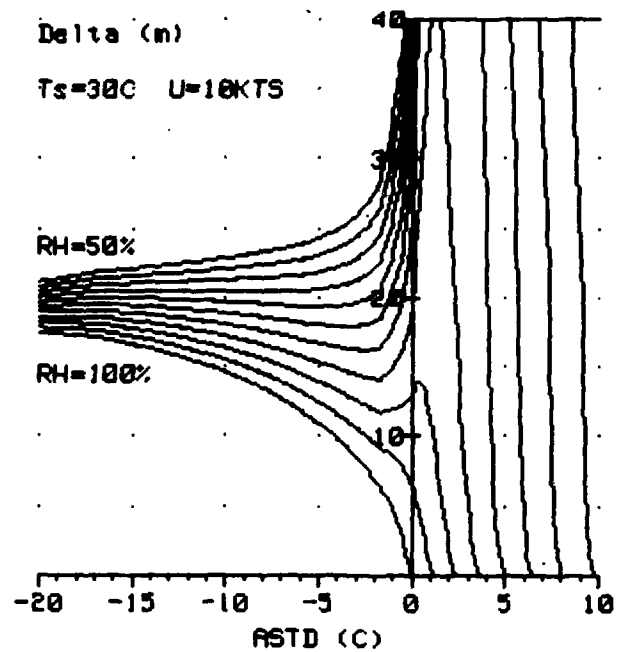
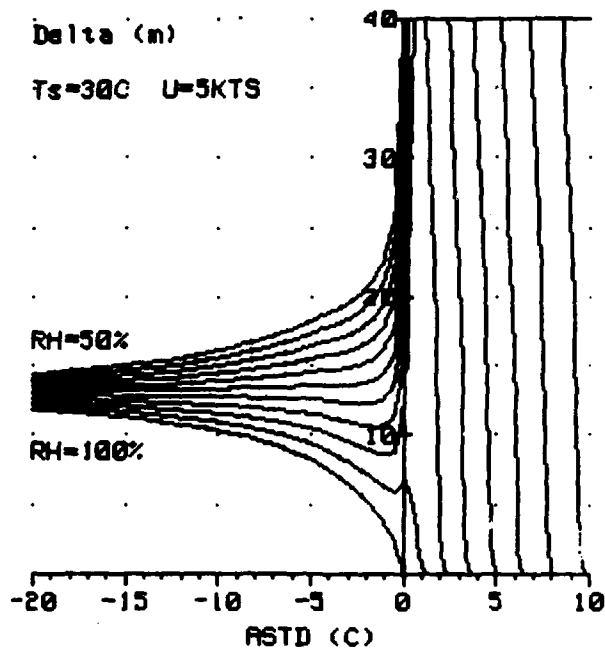


Figure 4a. Evaporation duct height (Delta) vs air-sea temperature difference (ASTD) parametric in relative humidity. $U = 5, 10, 15,$ and 20 knots wind speed and sea temperature, T_s , of 30°C .

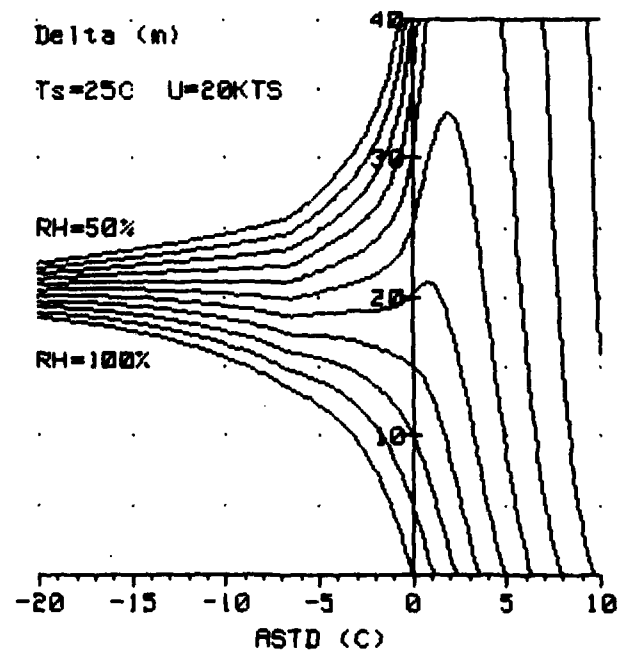
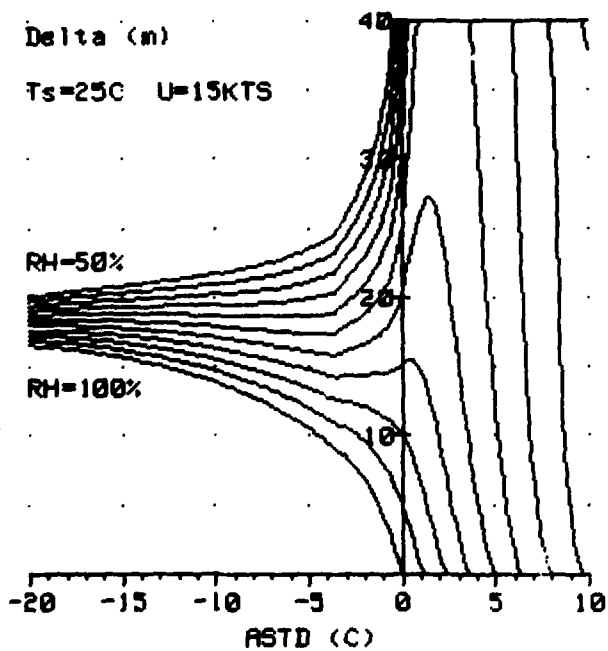
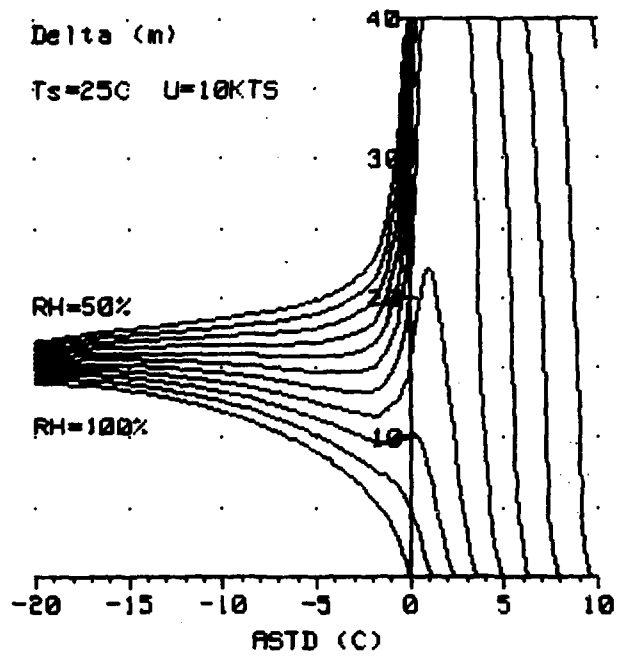
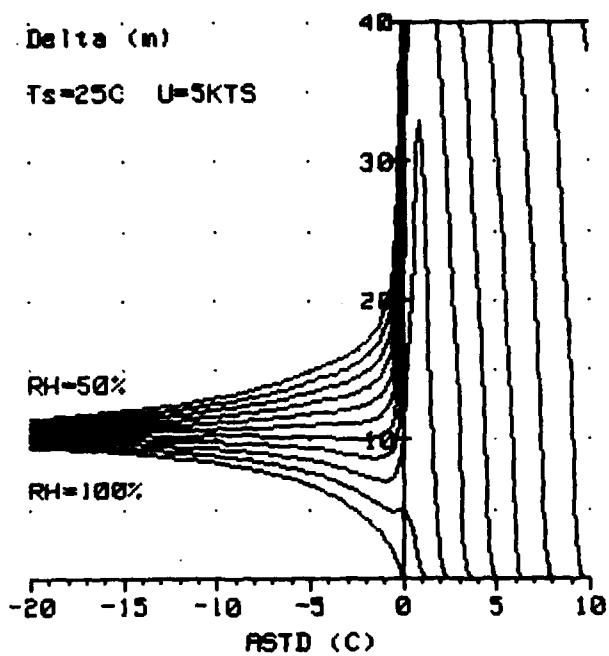


Figure 4b. Evaporation duct height (Delta) vs air-sea temperature difference (ASTD) parametric in relative humidity, U = 5, 10, 15, and 20 knots wind speed and sea temperature, T_s , of 25°C.

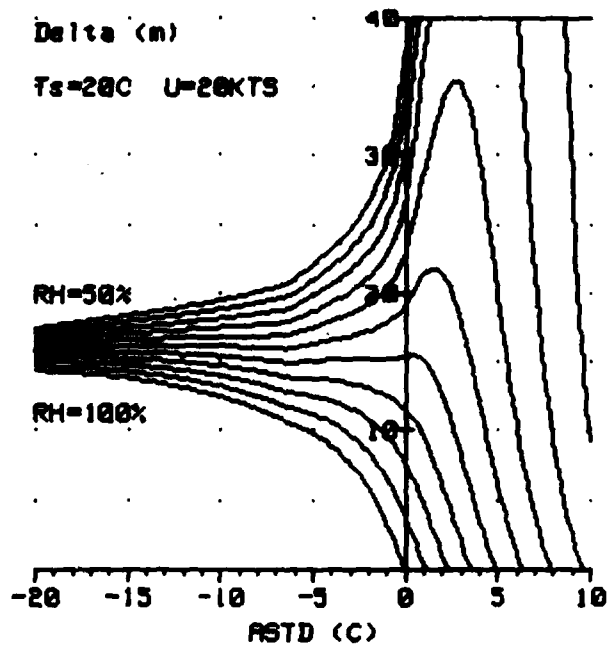
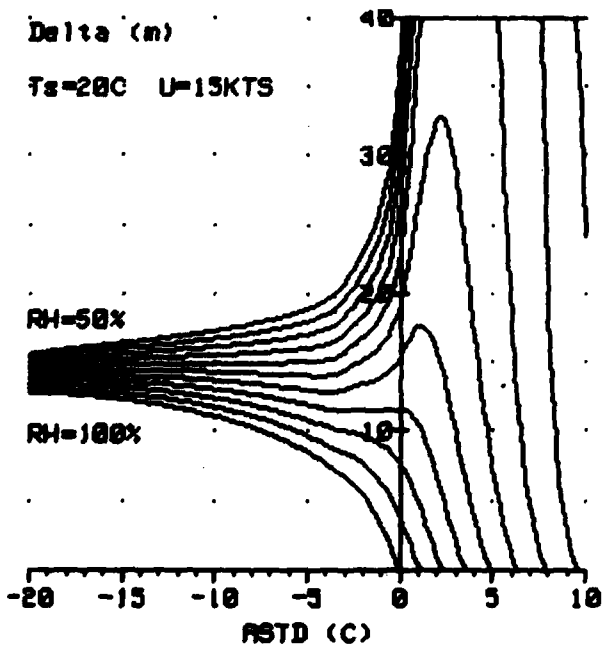
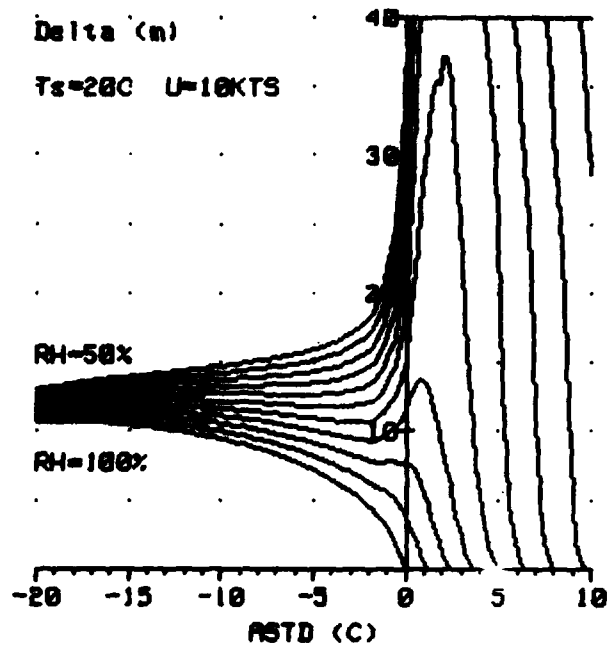
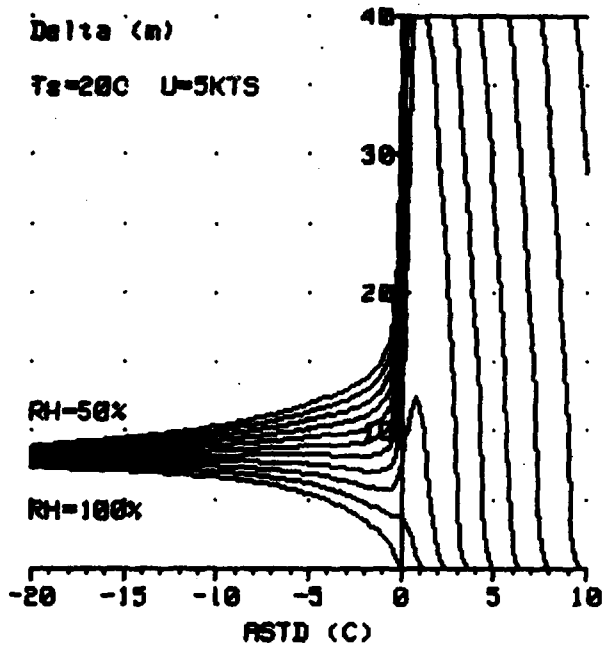


Figure 4c. Evaporation duct height (Delta) vs air-sea temperature difference (ASTD) parametric in relative humidity, $U = 5, 10, 15,$ and 20 knots wind speed and sea temperature, T_s , of $20^{\circ}C$.

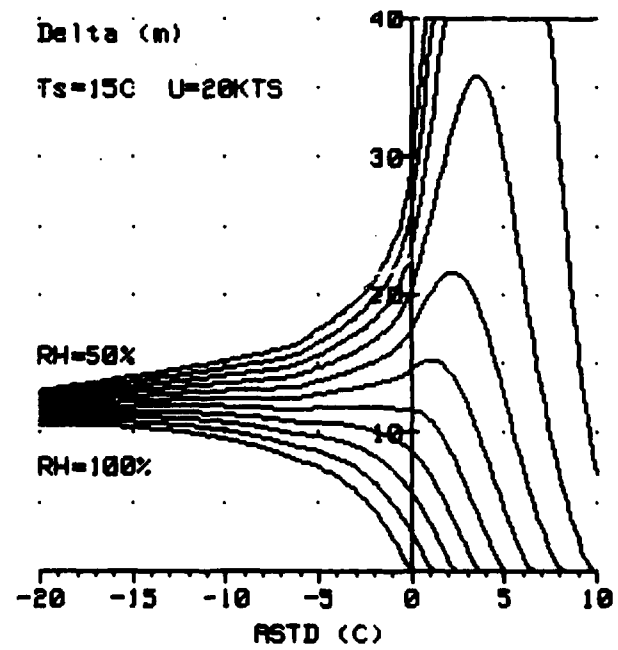
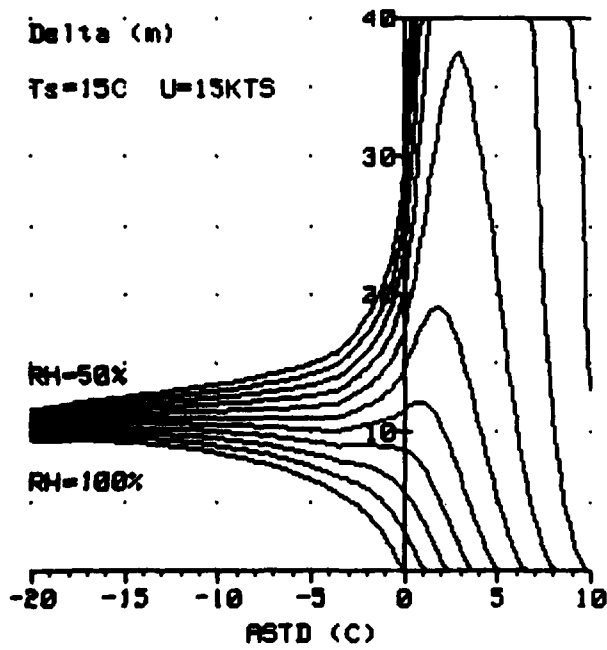
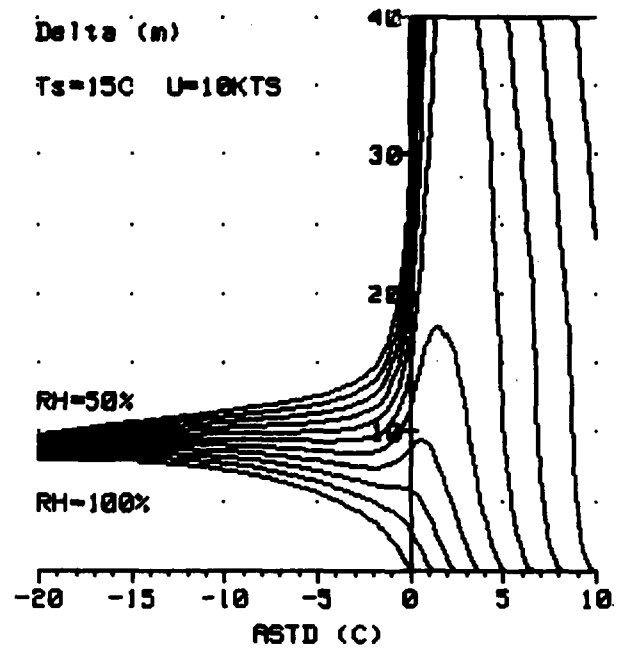
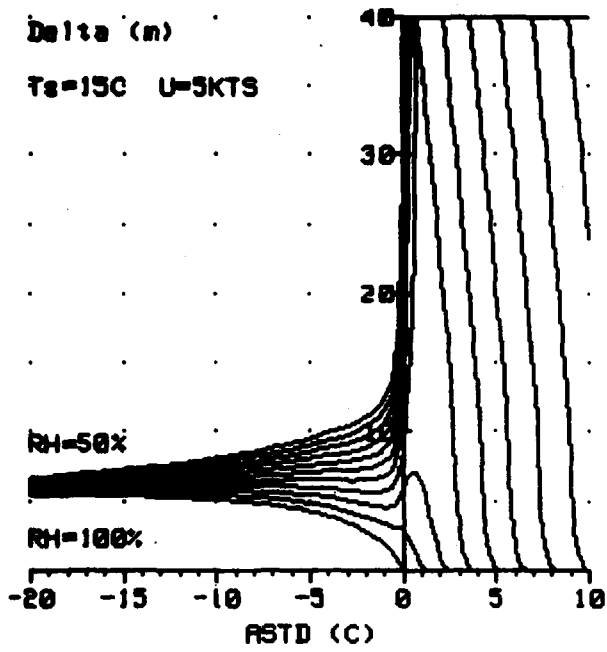


Figure 4d. Evaporation duct height (Delta) vs air-sea temperature difference (ASTD) parametric in relative humidity, U = 5, 10, 15, and 20 knots wind speed and sea temperature, T_s , of 15°C.

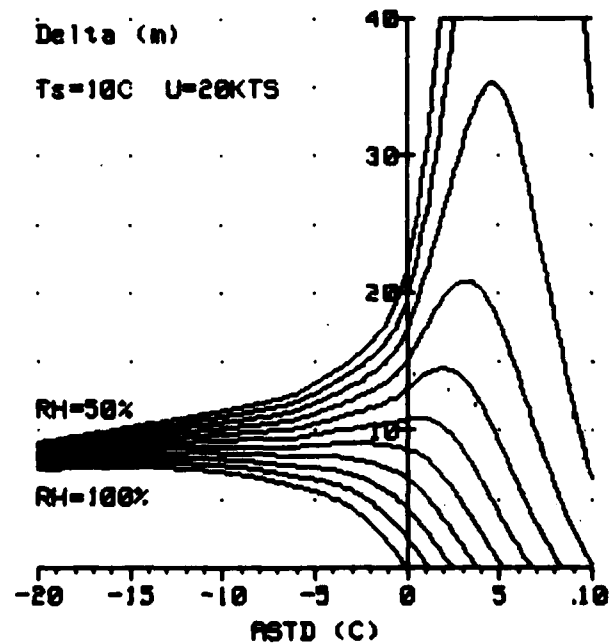
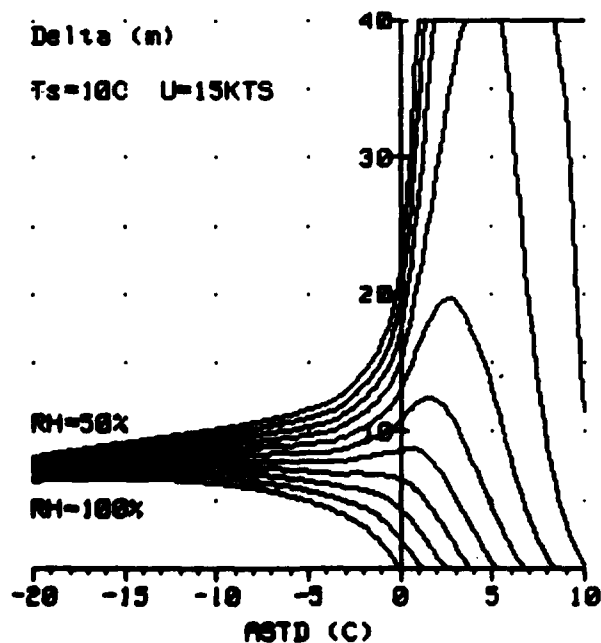
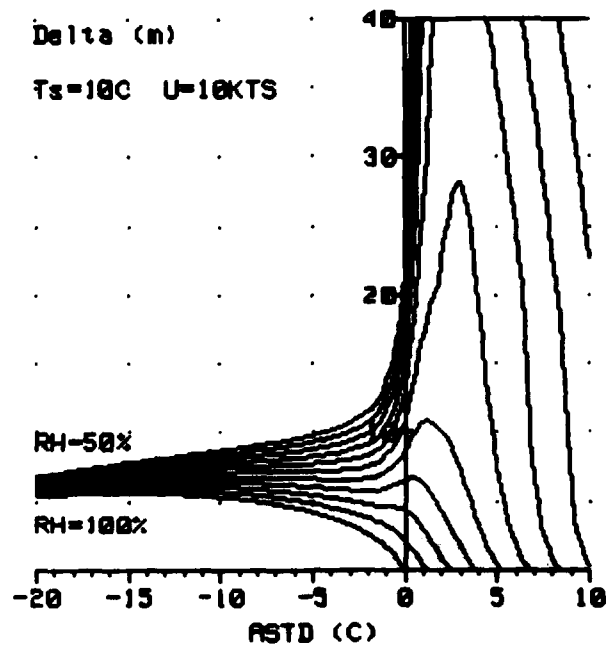
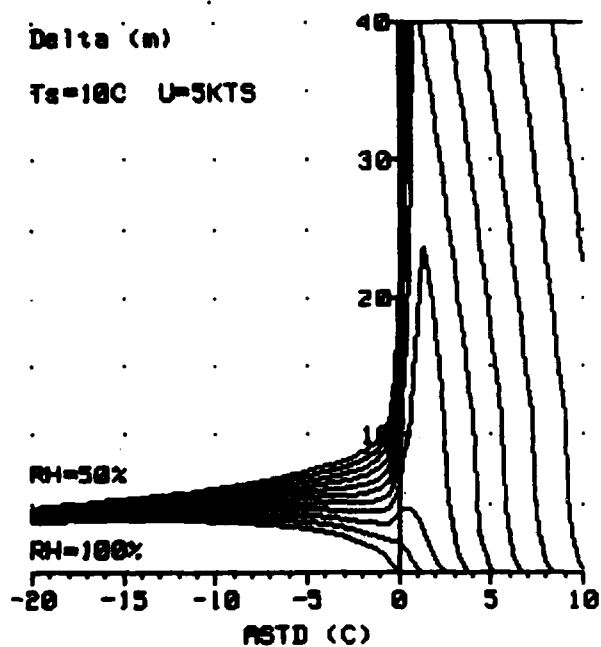


Figure 4e. Evaporation duct height (Delta) vs air-sea temperature difference (ASTD) parametric in relative humidity, $U = 5, 10, 15,$ and 20 knots wind speed and sea temperature, T_s , of 10°C .

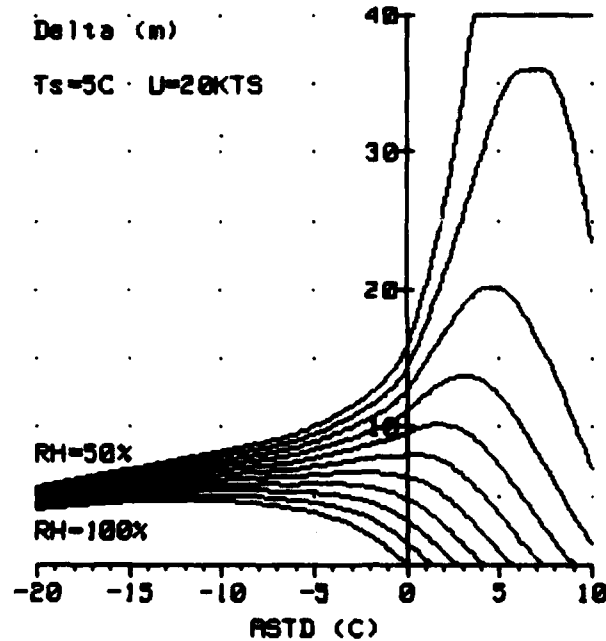
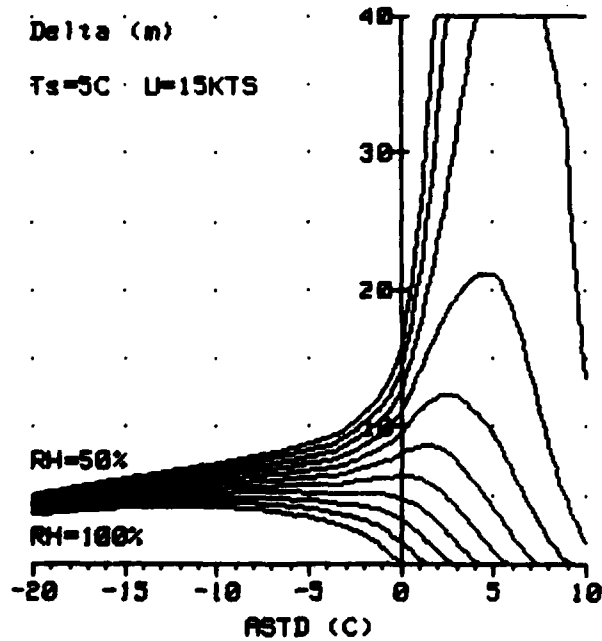
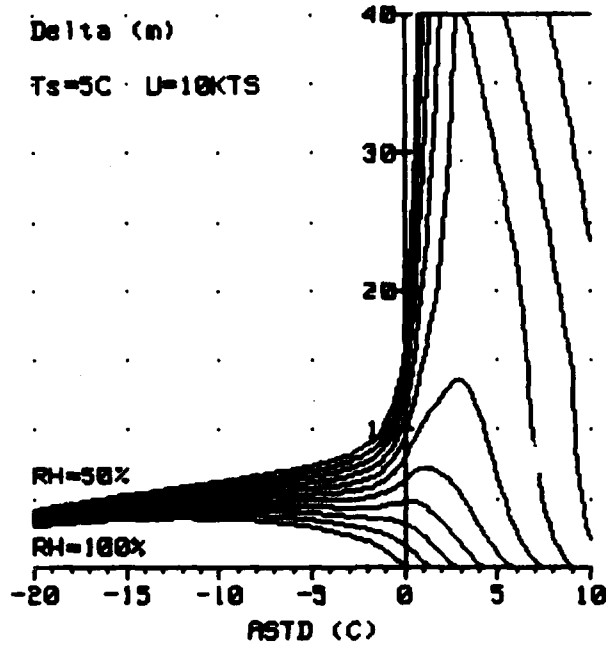
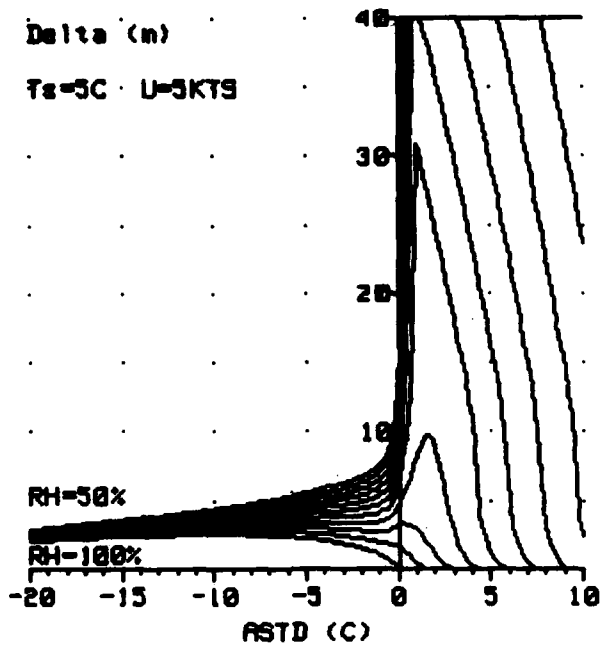


Figure 4f. Evaporation duct height (Delta) vs air-sea temperature difference (ASTD) parametric in relative humidity, U = 5, 10, 15, and 20 knots wind speed and sea temperature, T_s , of 5°C.

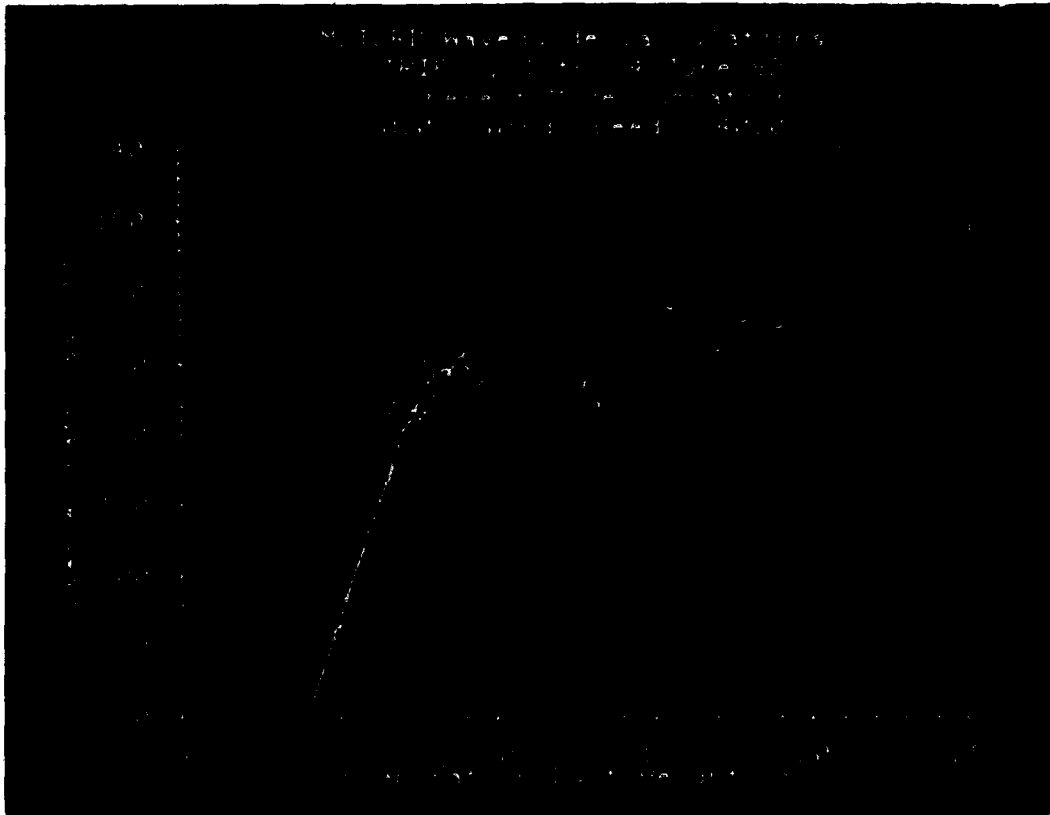


Figure 5a. RMS pathloss at 1.7 cm observed during the period 1-14 June 1982 vs calculated duct height (from reference 3). Solid lines are theoretical curves for bulk Richardson's number equal to -10, 0, and 0.1.

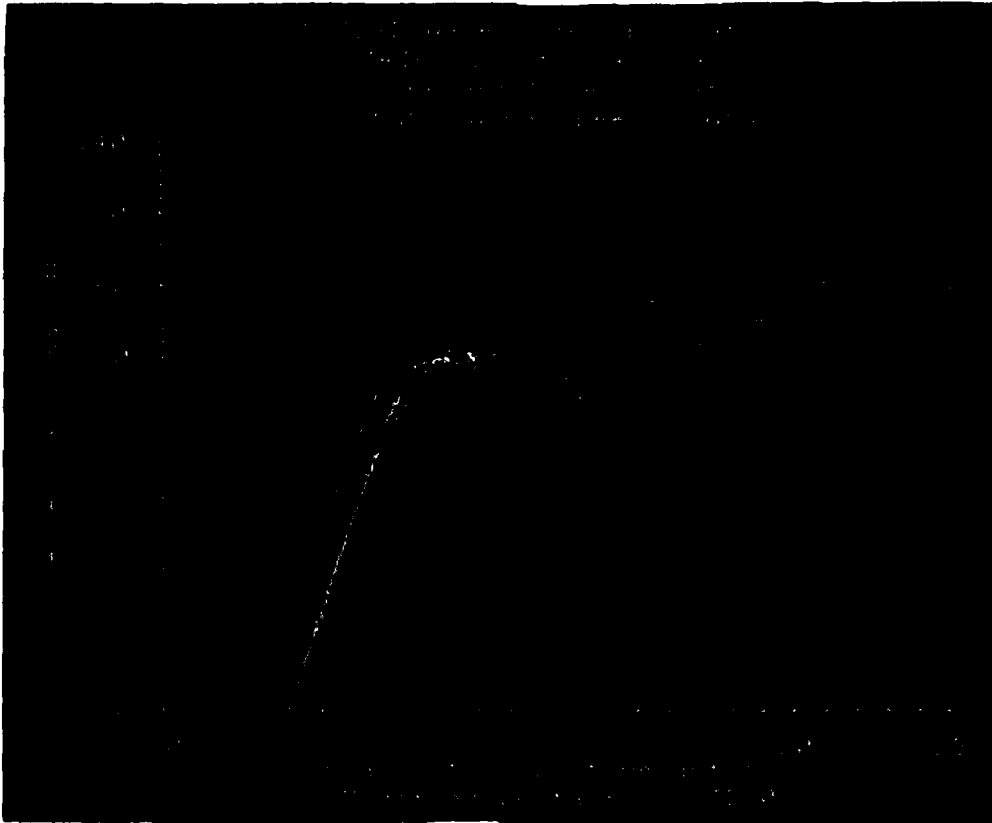


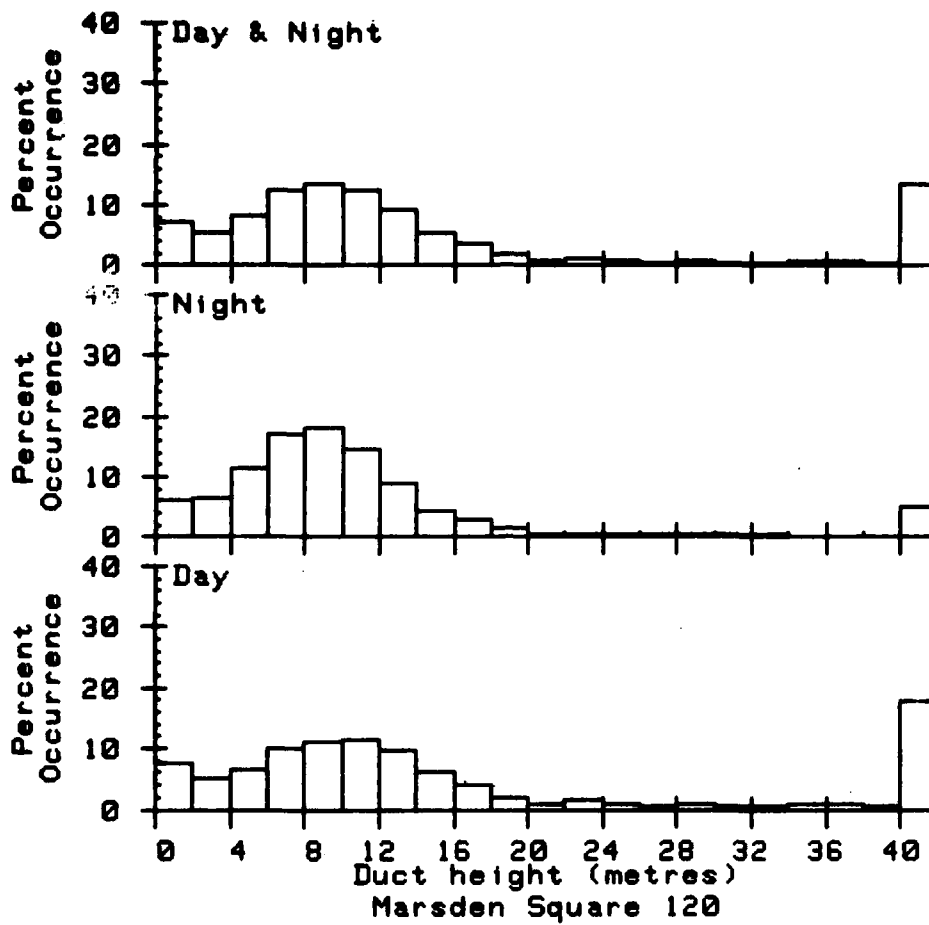
Figure 5b. Same as figure 5a, except a modified duct height calculation was used for air-sea temperature difference greater than 0.



Figure 5c. Same as figure 5b, except threshold used was for air-sea temperature difference greater than -0.5.

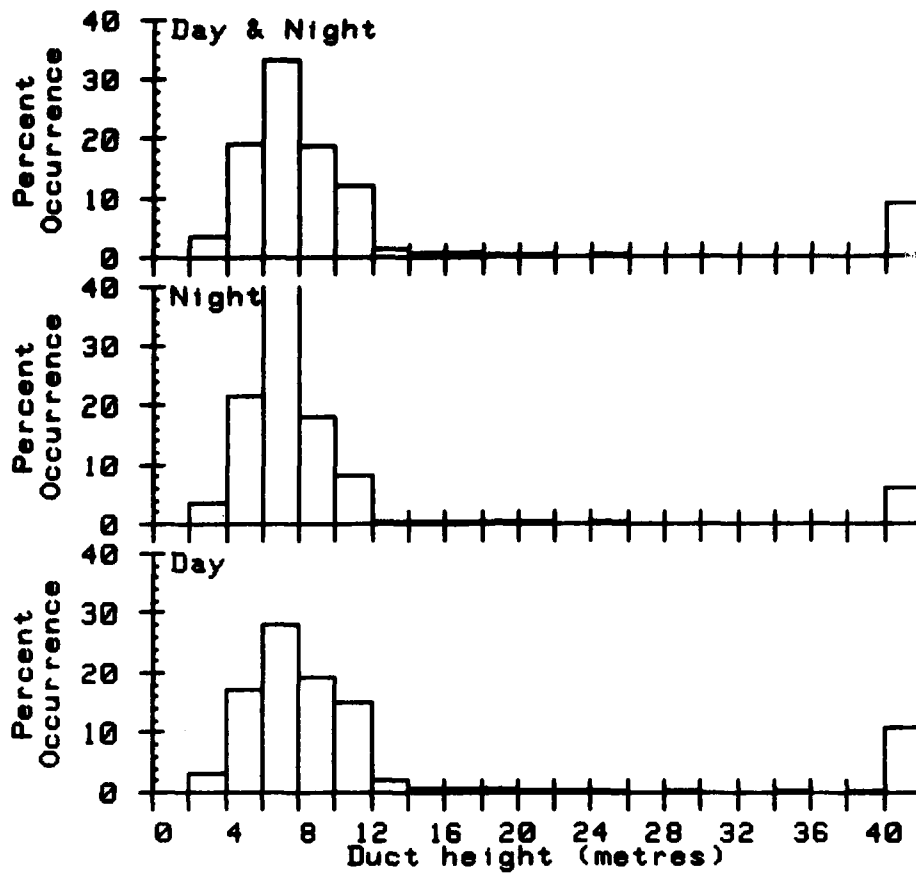


Figure 5d. Same as figure 5b, except threshold used was for air-sea temperature difference greater than -1.



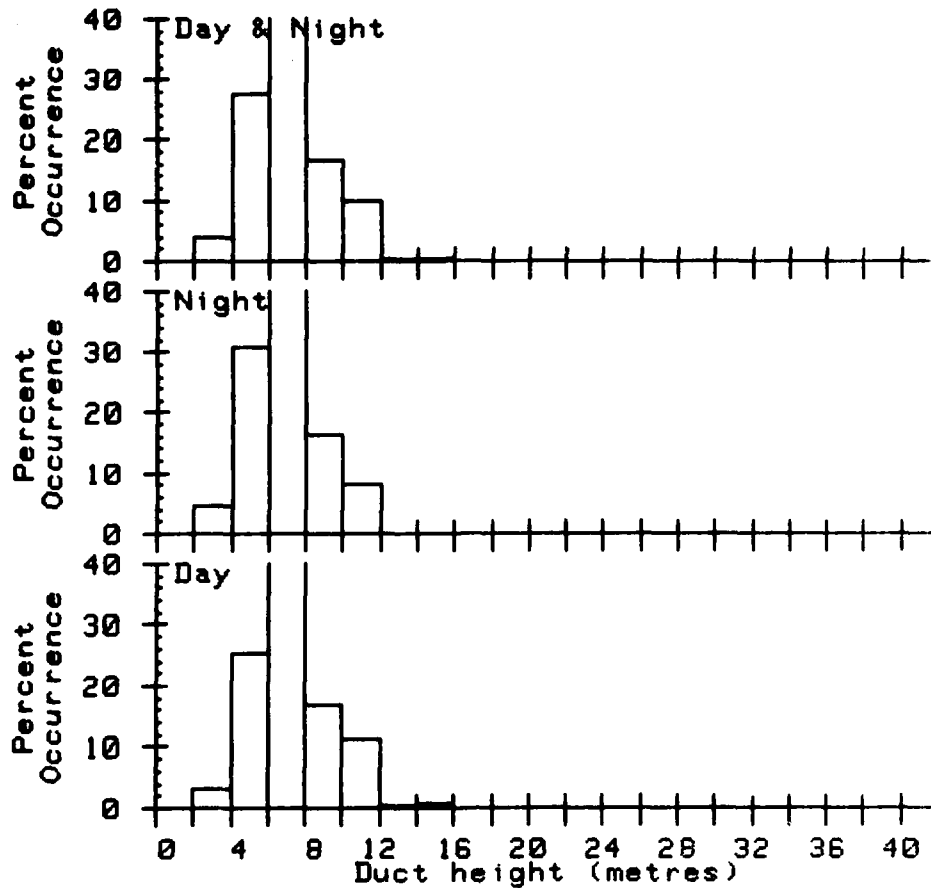
		% Occurrence			Cumulative % occurrence		
		Day	Night	D&N	Day	Night	D&N
LT	2	7.6	6.0	7.0	7.6	6.0	7.0
	4	5.1	6.5	5.5	12.6	12.5	12.6
	6	6.6	11.5	8.2	19.2	23.9	20.8
	8	10.1	17.0	12.4	29.3	40.9	33.1
	10	11.1	18.0	13.4	40.4	58.8	46.5
	12	11.6	14.5	12.6	52.0	73.3	59.1
	14	9.6	9.0	9.4	61.6	82.3	68.5
	16	6.1	4.5	5.5	67.7	86.8	74.0
	18	4.0	3.0	3.7	71.7	89.8	77.7
	20	2.0	1.5	1.8	73.7	91.2	79.5
	22	1.0	.5	.8	74.7	91.7	80.4
	24	1.5	.5	1.2	76.3	92.2	81.6
	26	1.0	.5	.8	77.3	92.7	82.4
	28	.5	.5	.5	77.8	93.2	82.9
	30	1.0	.5	.8	78.8	93.7	83.7
	32	.5	.5	.5	79.3	94.2	84.3
34	.5	.5	.5	79.8	94.7	84.8	
36	1.0	.1	.7	80.8	94.8	85.5	
38	1.0	.1	.7	81.8	94.9	86.2	
40	.5	.1	.4	82.3	95.0	86.5	
GT	40	17.7	5.0	13.5	100.0	100.0	100.0
Mean		19.3	11.8	16.8			
#Obs		2199	1078	3277			

Figure 6a. IREPS duct height climatology for Marsden square 120 for June.



LT	% Occurrence			Cumulative % occurrence		
	Day	Night	D&N	Day	Night	D&N
2	0.0	0.0	0.0	0.0	0.0	0.0
4	3.2	3.6	3.4	3.2	3.6	3.4
6	17.3	21.0	19.2	20.5	25.4	22.6
8	27.9	40.5	33.3	48.4	65.9	55.8
10	19.4	18.2	18.9	67.9	84.1	74.8
12	15.0	8.2	12.1	82.9	92.3	86.9
14	2.2	.2	1.3	85.0	92.5	88.2
16	.8	.3	.6	85.9	92.9	88.8
18	.8	.4	.6	86.7	93.2	89.5
20	.7	.2	.5	87.4	93.4	90.0
22	.3	.2	.3	87.7	93.6	90.2
24	.2	.1	.1	87.9	93.7	90.4
26	.2	.3	.2	88.1	93.9	90.6
28	.1	.1	.1	88.2	94.0	90.7
30	.2	0.0	.1	88.4	94.0	90.8
32	0.0	0.0	0.0	88.4	94.0	90.8
34	.1	0.0	.1	88.5	94.0	90.9
36	.2	0.0	.1	88.8	94.0	91.0
38	.1	0.0	.1	88.9	94.0	91.1
40	.2	0.0	.1	89.1	94.0	91.2
GT	100.0	100.0	100.0	100.0	100.0	100.0
Mean	13.2	9.7	11.7			
00bs	2100	1553	3653			

Figure 6b. Duct height distribution for June 1982 measurement period from reference 3.



LT		% Occurrence			Cumulative % occurrence		
		Day	Night	D&N	Day	Night	D&N
	2	0.0	0.0	0.0	0.0	0.0	0.0
	4	3.2	4.5	3.8	3.2	4.5	3.8
	6	25.2	30.7	27.5	28.4	35.2	31.3
	8	42.5	40.2	41.5	71.0	75.4	72.8
	10	16.7	16.4	16.5	87.6	91.8	89.4
	12	11.3	8.1	10.0	99.0	99.9	99.3
	14	.5	.1	.3	99.4	100.0	99.7
	16	.6	0.0	.3	100.0	100.0	100.0
	18	0.0	0.0	0.0	100.0	100.0	100.0
	20	0.0	0.0	0.0	100.0	100.0	100.0
	22	0.0	0.0	0.0	100.0	100.0	100.0
	24	0.0	0.0	0.0	100.0	100.0	100.0
	26	0.0	0.0	0.0	100.0	100.0	100.0
	28	0.0	0.0	0.0	100.0	100.0	100.0
	30	0.0	0.0	0.0	100.0	100.0	100.0
	32	0.0	0.0	0.0	100.0	100.0	100.0
	34	0.0	0.0	0.0	100.0	100.0	100.0
	36	0.0	0.0	0.0	100.0	100.0	100.0
	38	0.0	0.0	0.0	100.0	100.0	100.0
	40	0.0	0.0	0.0	100.0	100.0	100.0
GT	40	0.0	0.0	0.0	100.0	100.0	100.0
Mean		7.2	6.8	7.0			
#Obs		2100	1553	3653			

Figure 6c. Duct height distribution for June 1982 data after application of a modified duct height calculation.

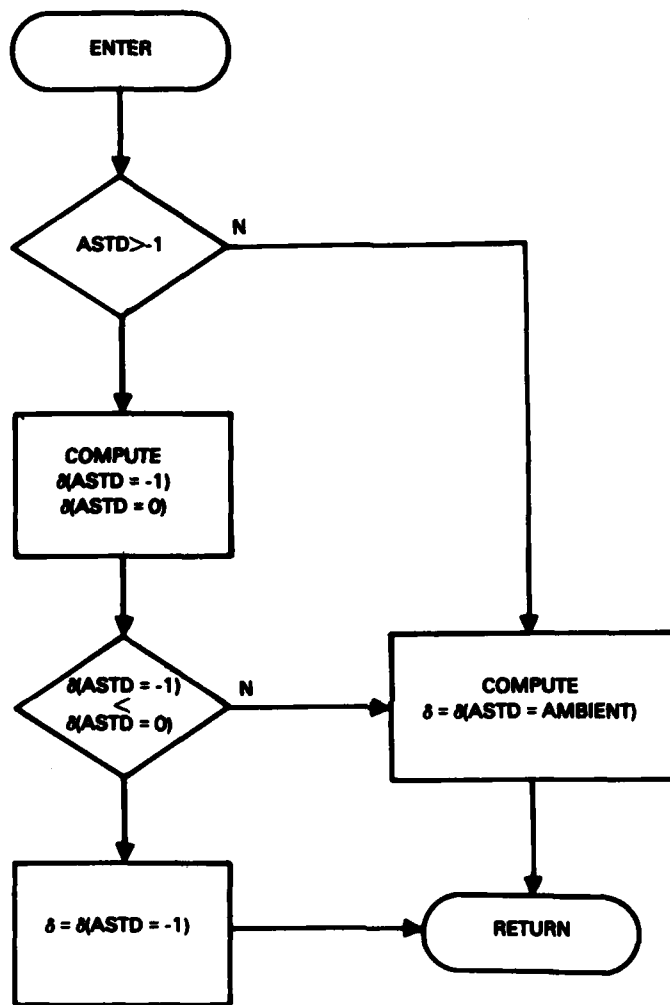


Figure 7. Flow chart for the modified evaporation duct calculation.

REFERENCES

1. Naval Oceanography Command Detachment Asheville, Evaporation Duct Report 76118, June 1981.
2. Patterson, W.L., Climatology of Marine Atmospheric Refractive Effects, NOSC TD 573, 20 December 1982.
3. Anderson, K.D., Evaporation Duct Effects on Moderate Range Propagation over the Sea at 10 and 1.7 cm Wavelengths, NOSC TR 858, 19 November 1982.
4. Director, Naval Oceanography and Meteorology, U.S. Navy Marine Climatic Atlas of the World, series.
5. Saur, J.F.T., A Study of the Quality of Sea Water Temperature Reported in Logs of Ships' Weather Observations, J. Appl. Meteor., 2, 417-425, 1963.
6. National Climatic Data Center, Climatic Summaries for NOAA Data Buoys, January 1983.
7. Gilhousen, D. B., NOAA Data Buoy Center, personal communication, January 1984.
8. Jeske, H., The State of Radar Range Prediction over Sea, Tropospheric Radio Wave Propagation - Part II, NATO-AGARD, February 1971.
9. Hitney, H.V., Propagation Modeling in the Evaporation Duct, NELC TR 1947, April 1975.
10. Anderson, K.D., Surface-Search Radar Performance in the Evaporation Duct: Global Predictions, NOSC TR 923, October 1983.

APPENDIX A

Histograms of Air-Sea Temperature Differences

for

**NOAA Data Buoys
and
IREPS Marsden Square Data**

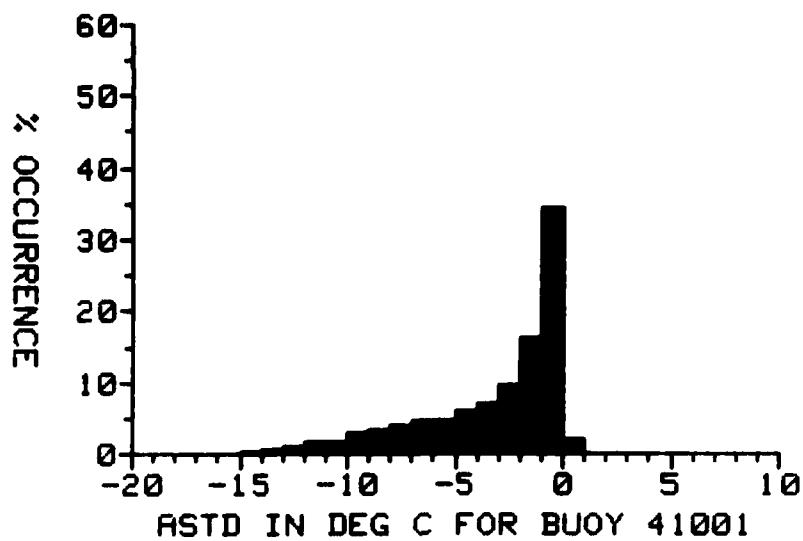
Annual Distributions

INTRODUCTION

This appendix contains the air-sea temperature difference distributions for the remaining NOAA data buoys and Marsden Squares. Table A-1 compares stable conditions. The remaining pages are the annual distributions. In particular, note the disparities between the Pacific buoys (which should be representative of open ocean conditions) and their respective Marsden squares.

Table A-1. Percent occurrence of stable conditions reported by NOAA data buoys as compared to Marsden square data from the IREPS historical data base.

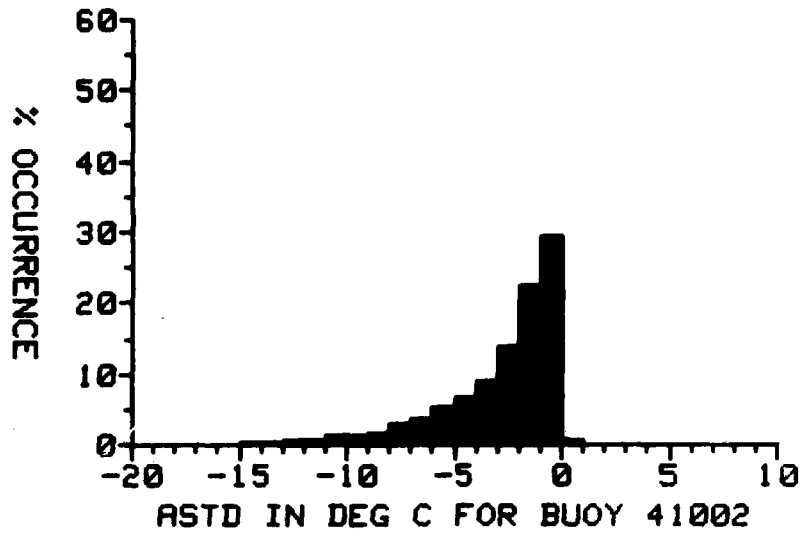
Buoy #	% occurrence of ASTD>0 for buoy	% occurrence of ASTD>0 for MS	Marsden square #
41001	2.1		
41002	0.6		
41004	4.1		
41005	4.5	32.0	116
44001	21.9		
44002	26.6		
44004	12.3		
44003	42.2		
44005	18.5	49.4	151
46002	1.6		
46005	4.6	51.0	158
46006	16.6		
46004	9.7	49.8	194
46001	3.0	54.1	195
46003	3.7	54.1	196



-20<#	obs<=-19	1	.01%
-19<#	obs<=-18	0	0.00%
-18<#	obs<=-17	6	.05%
-17<#	obs<=-16	4	.04%
-16<#	obs<=-15	15	.13%
-15<#	obs<=-14	33	.29%
-14<#	obs<=-13	82	.73%
-13<#	obs<=-12	122	1.08%
-12<#	obs<=-11	168	1.49%
-11<#	obs<=-10	194	1.72%
-10<#	obs<=-9	339	3.00%
-9<#	obs<=-8	359	3.18%
-8<#	obs<=-7	435	3.85%
-7<#	obs<=-6	538	4.76%
-6<#	obs<=-5	528	4.67%
-5<#	obs<=-4	684	6.05%
-4<#	obs<=-3	769	6.81%
-3<#	obs<=-2	1094	9.68%
-2<#	obs<=-1	1821	16.12%
-1<#	obs<= 0	3874	34.29%
0<#	obs<= 1	209	1.85%
1<#	obs<= 2	18	.16%
2<#	obs<= 3	5	.04%
3<#	obs<= 4	0	0.00%
4<#	obs<= 5	0	0.00%
5<#	obs<= 6	0	0.00%
6<#	obs<= 7	1	.01%

Total obs = 11299

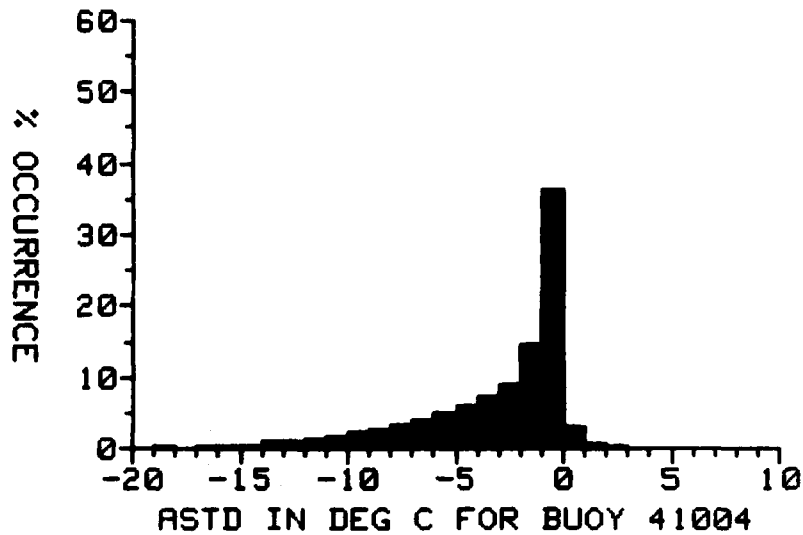
Figure A-1. Annual air-sea temperature difference distribution for buoy 41001 in Marsden square 118.



-19<#	obs<=-18	2	.01%
-18<#	obs<=-17	4	.01%
-17<#	obs<=-16	17	.06%
-16<#	obs<=-15	45	.15%
-15<#	obs<=-14	64	.21%
-14<#	obs<=-13	110	.36%
-13<#	obs<=-12	188	.61%
-12<#	obs<=-11	251	.82%
-11<#	obs<=-10	387	1.26%
-10<#	obs<= -9	433	1.41%
-9<#	obs<= -8	512	1.67%
-8<#	obs<= -7	923	3.01%
-7<#	obs<= -6	1084	3.53%
-6<#	obs<= -5	1653	5.39%
-5<#	obs<= -4	2022	6.59%
-4<#	obs<= -3	2708	8.82%
-3<#	obs<= -2	4211	13.72%
-2<#	obs<= -1	6869	22.38%
-1<#	obs<= 0	9028	29.39%
0<#	obs<= 1	178	.58%
1<#	obs<= 2	9	.03%

Total obs = 30690

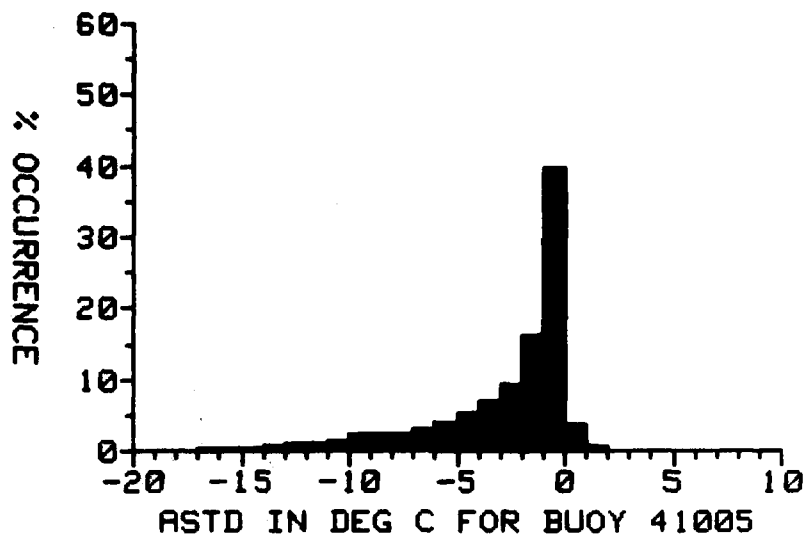
Figure A-2. Annual air-sea temperature difference distribution for buoy 41002 in Marsden square 116.



-22<#	obs<=-21	1	.00%
-21<#	obs<=-20	4	.02%
-20<#	obs<=-19	19	.09%
-19<#	obs<=-18	47	.21%
-18<#	obs<=-17	33	.15%
-17<#	obs<=-16	39	.18%
-16<#	obs<=-15	54	.24%
-15<#	obs<=-14	104	.47%
-14<#	obs<=-13	207	.93%
-13<#	obs<=-12	208	.94%
-12<#	obs<=-11	295	1.33%
-11<#	obs<=-10	332	1.49%
-10<#	obs<=-9	484	2.18%
-9<#	obs<=-8	591	2.66%
-8<#	obs<=-7	715	3.22%
-7<#	obs<=-6	877	3.95%
-6<#	obs<=-5	1124	5.06%
-5<#	obs<=-4	1344	6.05%
-4<#	obs<=-3	1586	7.14%
-3<#	obs<=-2	1992	8.96%
-2<#	obs<=-1	3228	14.52%
-1<#	obs<= 0	8041	36.18%
0<#	obs<= 1	674	3.03%
1<#	obs<= 2	158	.71%
2<#	obs<= 3	62	.28%
3<#	obs<= 4	6	.03%
4<#	obs<= 5	2	.01%

Total obs = 22227

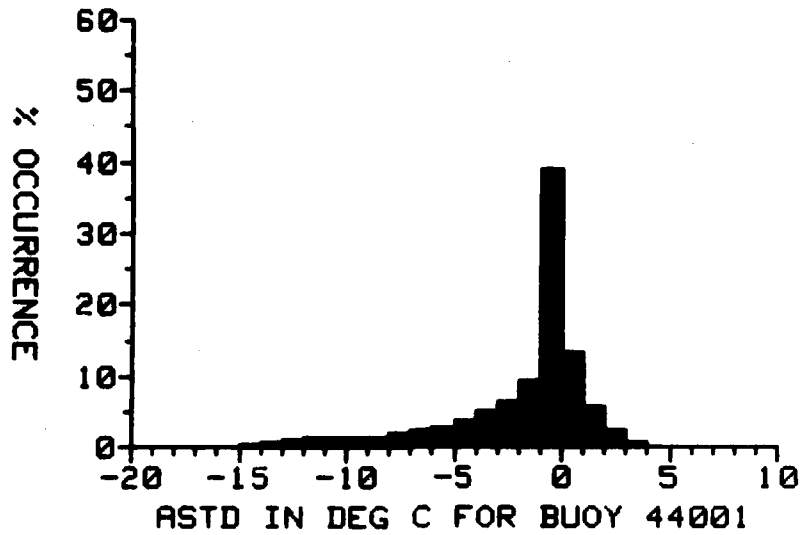
Figure A-3. Annual air-sea temperature difference distribution for buoy 41004 in Marsden square 116.



-21<#	obs<=-20	1	.00%
-20<#	obs<=-19	7	.03%
-19<#	obs<=-18	25	.12%
-18<#	obs<=-17	32	.15%
-17<#	obs<=-16	44	.21%
-16<#	obs<=-15	76	.36%
-15<#	obs<=-14	82	.38%
-14<#	obs<=-13	140	.66%
-13<#	obs<=-12	187	.88%
-12<#	obs<=-11	221	1.03%
-11<#	obs<=-10	269	1.26%
-10<#	obs<= -9	481	2.25%
-9<#	obs<= -8	471	2.20%
-8<#	obs<= -7	495	2.32%
-7<#	obs<= -6	627	2.94%
-6<#	obs<= -5	835	3.91%
-5<#	obs<= -4	1104	5.17%
-4<#	obs<= -3	1460	6.83%
-3<#	obs<= -2	1977	9.26%
-2<#	obs<= -1	3438	16.09%
-1<#	obs<= 0	8420	39.42%
0<#	obs<= 1	798	3.74%
1<#	obs<= 2	143	.67%
2<#	obs<= 3	28	.13%

Total obs = 21361

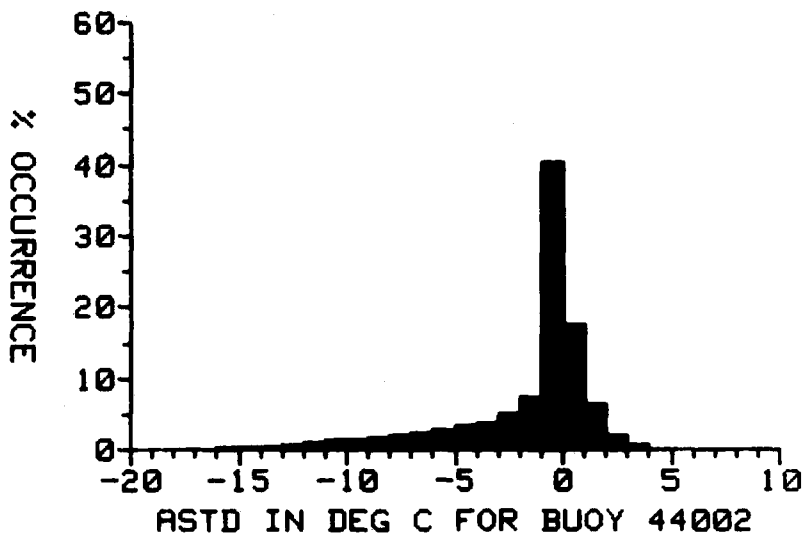
Figure A-4. Annual air-sea temperature difference distribution for buoy 41005 in Meraden square 116.



-18<#	obs<=-17	3	.01%
-17<#	obs<=-16	33	.13%
-16<#	obs<=-15	36	.14%
-15<#	obs<=-14	111	.44%
-14<#	obs<=-13	193	.77%
-13<#	obs<=-12	222	.89%
-12<#	obs<=-11	326	1.30%
-11<#	obs<=-10	333	1.33%
-10<#	obs<=-9	335	1.34%
-9<#	obs<=-8	359	1.44%
-8<#	obs<=-7	499	2.00%
-7<#	obs<=-6	608	2.43%
-6<#	obs<=-5	690	2.76%
-5<#	obs<=-4	941	3.77%
-4<#	obs<=-3	1197	4.79%
-3<#	obs<=-2	1582	6.33%
-2<#	obs<=-1	2315	9.27%
-1<#	obs<= 0	9723	38.92%
0<#	obs<= 1	3298	13.20%
1<#	obs<= 2	1391	5.57%
2<#	obs<= 3	586	2.35%
3<#	obs<= 4	160	.64%
4<#	obs<= 5	35	.14%
5<#	obs<= 6	8	.03%

Total obs = 24984

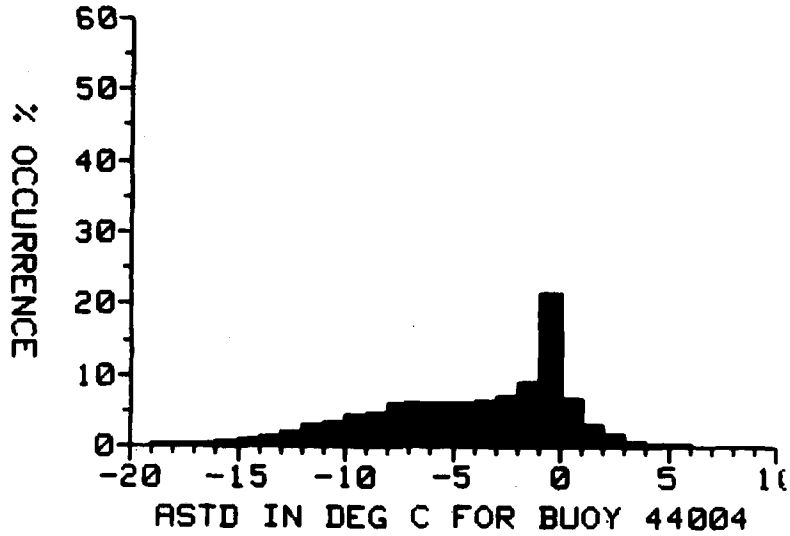
Figure A-5. Annual air-sea temperature difference distribution for buoy 44001 in Marsden square 116.



-18<#	obs<=-17	8	.02%
-17<#	obs<=-16	31	.10%
-16<#	obs<=-15	63	.19%
-15<#	obs<=-14	130	.40%
-14<#	obs<=-13	136	.42%
-13<#	obs<=-12	233	.72%
-12<#	obs<=-11	293	.91%
-11<#	obs<=-10	374	1.16%
-10<#	obs<= -9	439	1.36%
-9<#	obs<= -8	539	1.67%
-8<#	obs<= -7	656	2.03%
-7<#	obs<= -6	777	2.40%
-6<#	obs<= -5	803	2.48%
-5<#	obs<= -4	1056	3.26%
-4<#	obs<= -3	1223	3.70%
-3<#	obs<= -2	1580	4.88%
-2<#	obs<= -1	2385	7.37%
-1<#	obs<= 0	13015	40.22%
0<#	obs<= 1	5674	17.53%
1<#	obs<= 2	2071	6.40%
2<#	obs<= 3	621	1.92%
3<#	obs<= 4	217	.67%
4<#	obs<= 5	33	.10%
5<#	obs<= 6	3	.01%

Total obs = 32360

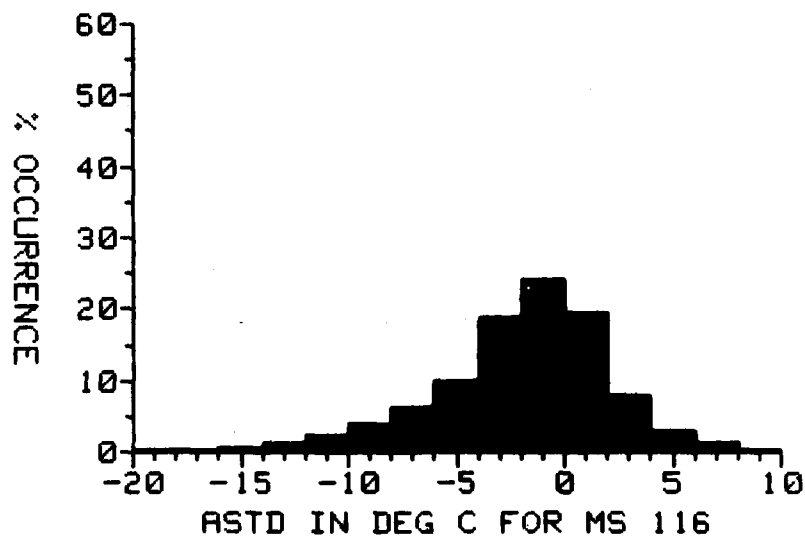
Figure A-6. Annual air-sea temperature difference distribution for buoy 44002 in Marsden square 116.



-23<#	obs<=-22	9	.05%
-22<#	obs<=-21	12	.06%
-21<#	obs<=-20	13	.07%
-20<#	obs<=-19	11	.06%
-19<#	obs<=-18	39	.21%
-18<#	obs<=-17	74	.40%
-17<#	obs<=-16	78	.42%
-16<#	obs<=-15	111	.60%
-15<#	obs<=-14	178	.96%
-14<#	obs<=-13	239	1.29%
-13<#	obs<=-12	362	1.96%
-12<#	obs<=-11	527	2.85%
-11<#	obs<=-10	623	3.37%
-10<#	obs<= -9	764	4.13%
-9<#	obs<= -8	879	4.75%
-8<#	obs<= -7	1069	5.78%
-7<#	obs<= -6	1096	5.93%
-6<#	obs<= -5	1093	5.91%
-5<#	obs<= -4	1067	5.77%
-4<#	obs<= -3	1147	6.20%
-3<#	obs<= -2	1250	6.76%
-2<#	obs<= -1	1625	8.79%
-1<#	obs<= 0	3954	21.38%
0<#	obs<= 1	1198	6.44%
1<#	obs<= 2	538	2.91%
2<#	obs<= 3	288	1.56%
3<#	obs<= 4	143	.77%
4<#	obs<= 5	76	.41%
5<#	obs<= 6	31	.17%
6<#	obs<= 7	6	.03%

Total obs = 18492

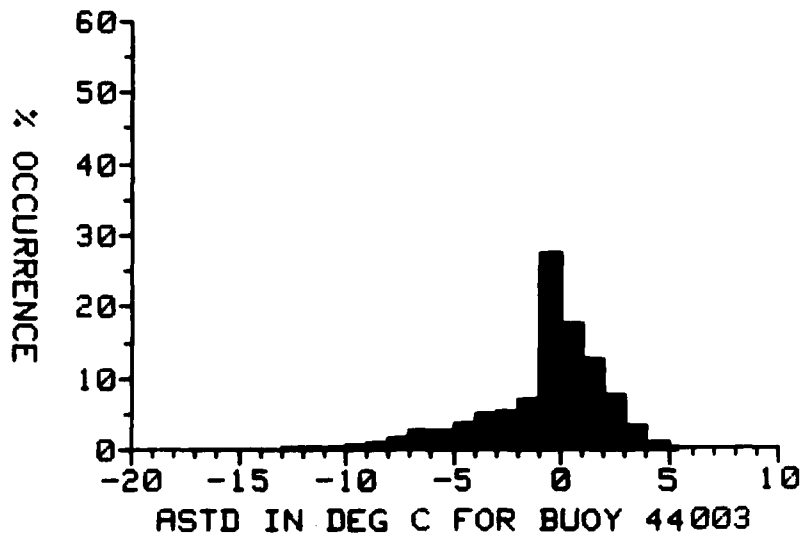
Figure A-7. Annual air-sea temperature difference distribution for buoy 44004 in Marsden square 116.



-22<#	obs<=-20	176	.08%
-20<#	obs<=-18	441	.20%
-18<#	obs<=-16	882	.40%
-16<#	obs<=-14	1631	.74%
-14<#	obs<=-12	3130	1.42%
-12<#	obs<=-10	4849	2.20%
-10<#	obs<= -8	8486	3.85%
-8<#	obs<= -6	13754	6.24%
-6<#	obs<= -4	21887	9.94%
-4<#	obs<= -2	41679	18.92%
-2<#	obs<= 0	52942	24.04%
0<#	obs<= 2	42870	19.46%
2<#	obs<= 4	17148	7.79%
4<#	obs<= 6	6238	2.83%
6<#	obs<= 8	2711	1.23%
8<#	obs<= 10	926	.42%
10<#	obs<= 12	353	.16%
12<#	obs<= 14	132	.06%
14<#	obs<= 16	22	.01%

Total obs = 220255

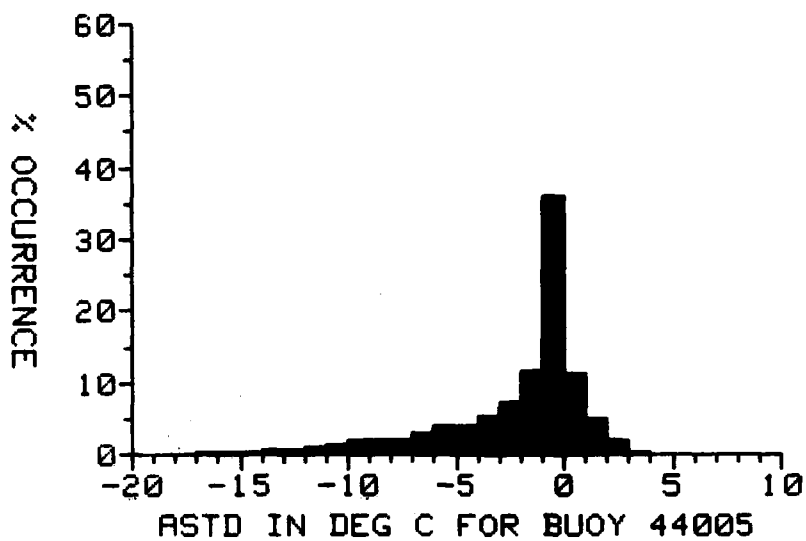
Figure A-8. Annual air-sea temperature difference distribution for Marsden square 116 from IREPS historical data base. Compare with distributions in figures A-1 through A-7.



-18<#	obs<=-17	5	.02%
-17<#	obs<=-16	6	.02%
-16<#	obs<=-15	18	.06%
-15<#	obs<=-14	17	.06%
-14<#	obs<=-13	26	.08%
-13<#	obs<=-12	52	.17%
-12<#	obs<=-11	83	.27%
-11<#	obs<=-10	128	.42%
-10<#	obs<=-9	237	.77%
-9<#	obs<=-8	323	1.05%
-8<#	obs<=-7	485	1.58%
-7<#	obs<=-6	797	2.60%
-6<#	obs<=-5	844	2.75%
-5<#	obs<=-4	1151	3.76%
-4<#	obs<=-3	1518	4.95%
-3<#	obs<=-2	1604	5.24%
-2<#	obs<=-1	2093	6.83%
-1<#	obs<= 0	8333	27.20%
0<#	obs<= 1	5343	17.44%
1<#	obs<= 2	3055	12.58%
2<#	obs<= 3	2338	7.63%
3<#	obs<= 4	1001	3.27%
4<#	obs<= 5	283	.92%
5<#	obs<= 6	87	.28%
6<#	obs<= 7	7	.02%
7<#	obs<= 8	2	.01%

Total obs = 30636

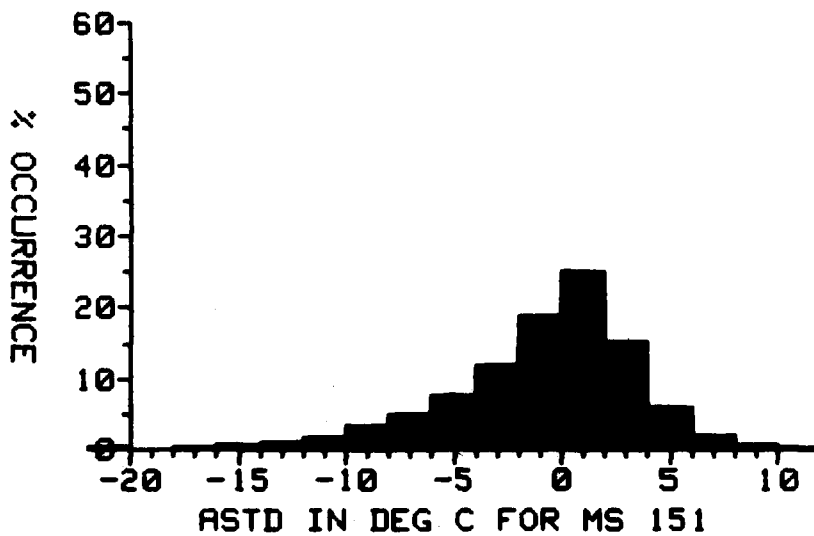
Figure A-9. Annual air-sea temperature difference distribution for buoy 44003 in Marsden square 151.



-21<#	obs<=-20	8	.04%
-20<#	obs<=-19	7	.04%
-19<#	obs<=-18	21	.12%
-18<#	obs<=-17	18	.10%
-17<#	obs<=-16	36	.20%
-16<#	obs<=-15	56	.31%
-15<#	obs<=-14	76	.42%
-14<#	obs<=-13	105	.58%
-13<#	obs<=-12	133	.74%
-12<#	obs<=-11	206	1.14%
-11<#	obs<=-10	211	1.17%
-10<#	obs<=-9	334	1.85%
-9<#	obs<=-8	354	1.96%
-8<#	obs<=-7	361	2.00%
-7<#	obs<=-6	555	3.07%
-6<#	obs<=-5	690	3.82%
-5<#	obs<=-4	708	3.92%
-4<#	obs<=-3	968	5.36%
-3<#	obs<=-2	1305	7.23%
-2<#	obs<=-1	2090	11.57%
-1<#	obs<= 0	6469	35.82%
0<#	obs<= 1	2053	11.37%
1<#	obs<= 2	867	4.80%
2<#	obs<= 3	344	1.90%
3<#	obs<= 4	62	.34%
4<#	obs<= 5	14	.08%
5<#	obs<= 6	8	.04%
6<#	obs<= 7	2	.01%

Total obs = 18061

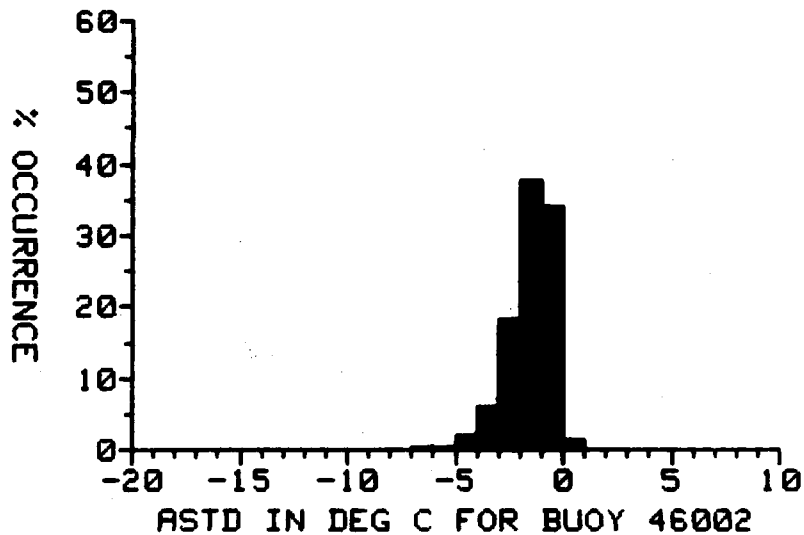
Figure A-10. Annual air-sea temperature difference distribution for buoy 44005 in Marsden square 151.



-22<#	obs<=-20	162	.19%
-20<#	obs<=-18	182	.12%
-18<#	obs<=-16	295	.24%
-16<#	obs<=-14	487	.57%
-14<#	obs<=-12	985	1.06%
-12<#	obs<=-10	1529	1.78%
-10<#	obs<=-8	2927	3.30%
-8<#	obs<=-6	4321	5.04%
-6<#	obs<=-4	6431	7.50%
-4<#	obs<=-2	10197	11.89%
-2<#	obs<= 0	16166	18.86%
0<#	obs<= 2	21606	25.20%
2<#	obs<= 4	12861	15.00%
4<#	obs<= 6	5881	5.93%
6<#	obs<= 8	1810	2.11%
8<#	obs<= 10	606	.71%
10<#	obs<= 12	248	.29%
12<#	obs<= 14	85	.10%
14<#	obs<= 16	51	.06%
16<#	obs<= 18	9	.01%
18<#	obs<= 20	9	.01%
20<#	obs<= 22	26	.03%

Total obs = 85725

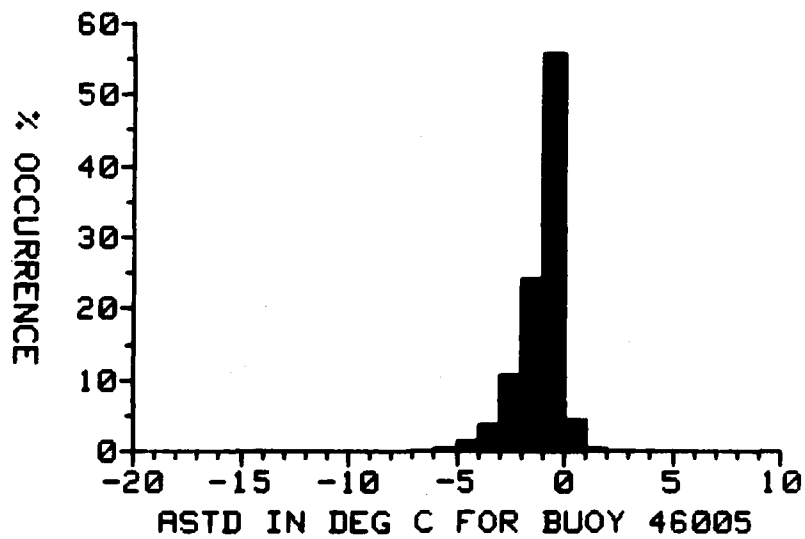
Figure A-11. Annual air-sea temperature difference distribution for Mersden square 151 from IREPS historical data base. Compare with distribution in figures A-9 and A-10.



-9<# obs<= -8	4	.01%
-8<# obs<= -7	21	.06%
-7<# obs<= -6	63	.17%
-6<# obs<= -5	158	.43%
-5<# obs<= -4	701	1.93%
-4<# obs<= -3	2139	5.88%
-3<# obs<= -2	6650	18.29%
-2<# obs<= -1	13628	37.49%
-1<# obs<= 0	12388	34.08%
0<# obs<= 1	536	1.47%
1<# obs<= 2	58	.16%
2<# obs<= 3	5	.01%

Total obs = 36351

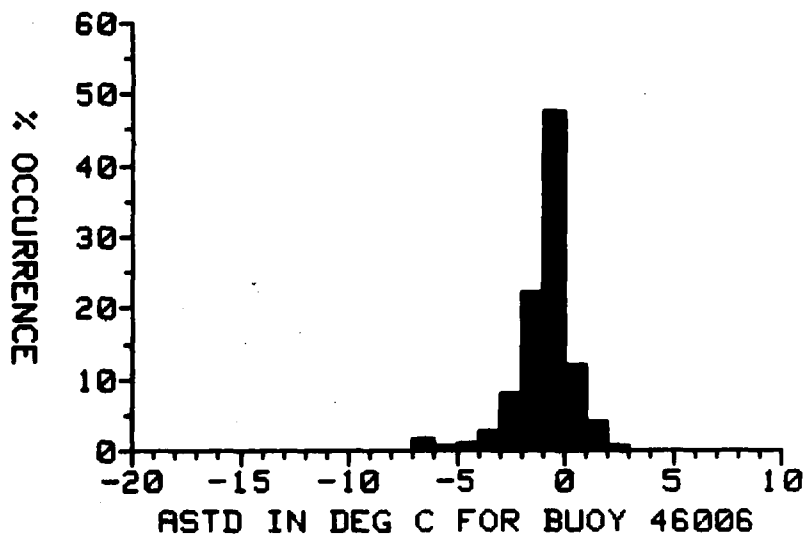
Figure A-12. Annual air-sea temperature difference distribution for buoy 46002 in Marsden square 158.



-10<# obs<= -9	2	.01%
-9<# obs<= -8	1	.00%
-8<# obs<= -7	8	.02%
-7<# obs<= -6	42	.13%
-6<# obs<= -5	134	.41%
-5<# obs<= -4	413	1.26%
-4<# obs<= -3	1135	3.48%
-3<# obs<= -2	3447	10.55%
-2<# obs<= -1	7814	23.93%
-1<# obs<= 0	18176	55.65%
0<# obs<= 1	1372	4.20%
1<# obs<= 2	111	.34%
2<# obs<= 3	3	.01%
3<# obs<= 4	0	0.00%
4<# obs<= 5	1	.00%

Total obs = 32659

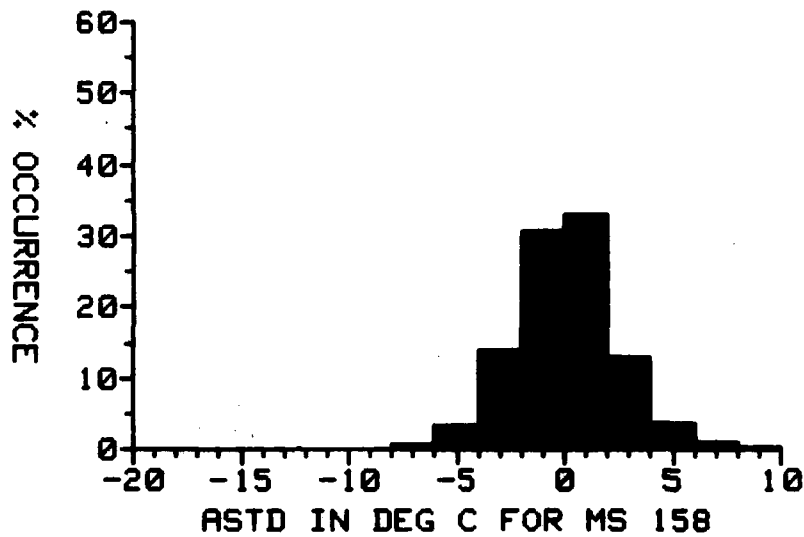
Figure A-13. Annual air-sea temperature difference distribution for buoy 46005 in Marsden square 158.



-9<# obs<= -8	1	.01%
-8<# obs<= -7	9	.06%
-7<# obs<= -6	255	1.67%
-6<# obs<= -5	98	.64%
-5<# obs<= -4	140	.92%
-4<# obs<= -3	425	2.78%
-3<# obs<= -2	1218	7.96%
-2<# obs<= -1	3356	21.94%
-1<# obs<= 0	7249	47.39%
0<# obs<= 1	1804	11.79%
1<# obs<= 2	610	3.99%
2<# obs<= 3	122	.80%
3<# obs<= 4	8	.05%

Total obs = 15295

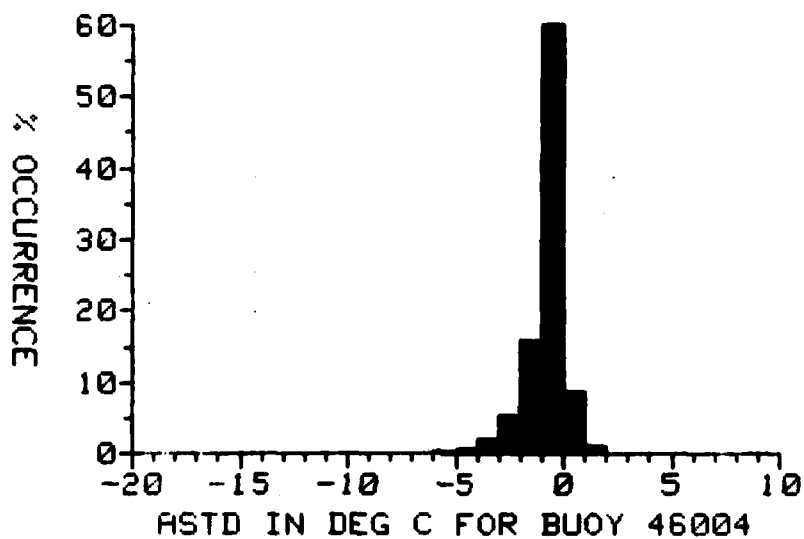
Figure A-14. Annual air-sea temperature difference distribution for buoy 46006 in Marsden square 158.



-12<# obs<=-10	7	.01%
-10<# obs<= -8	93	.14%
-8<# obs<= -6	484	.73%
-6<# obs<= -4	2223	3.35%
-4<# obs<= -2	9283	13.99%
-2<# obs<= 0	20430	30.60%
0<# obs<= 2	21764	32.81%
2<# obs<= 4	8546	12.88%
4<# obs<= 6	2495	3.76%
6<# obs<= 8	697	1.05%
8<# obs<= 10	226	.34%
10<# obs<= 12	73	.11%
12<# obs<= 14	20	.03%

Total obs = 66340

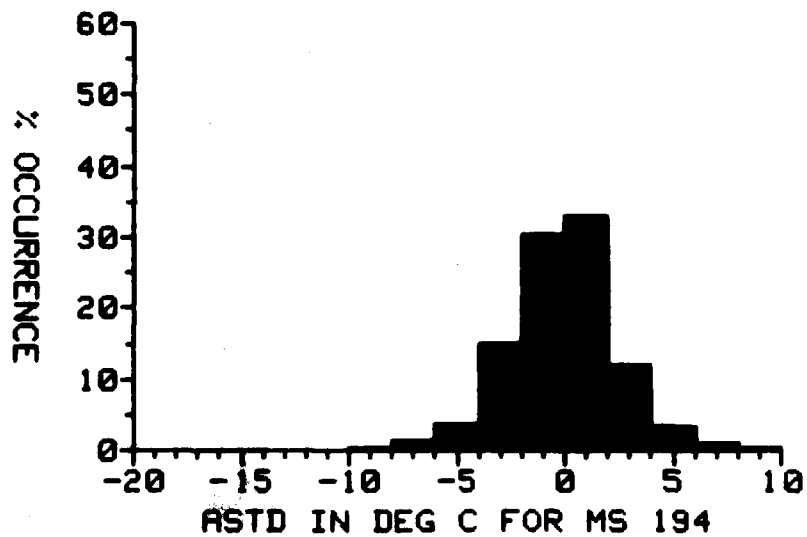
Figure A-15. Annual air-sea temperature difference distribution for Maraden square 158 from IREPS historical data base. Compare with distribution in figures A-12 through A-14.



-9<# obs<= -8	1	.00%
-8<# obs<= -7	4	.01%
-7<# obs<= -6	35	.12%
-6<# obs<= -5	110	.38%
-5<# obs<= -4	214	.74%
-4<# obs<= -3	614	2.11%
-3<# obs<= -2	1553	5.35%
-2<# obs<= -1	4595	15.83%
-1<# obs<= 0	19100	65.78%
0<# obs<= 1	2493	8.59%
1<# obs<= 2	310	1.07%
2<# obs<= 3	5	.02%

Total obs = 29034

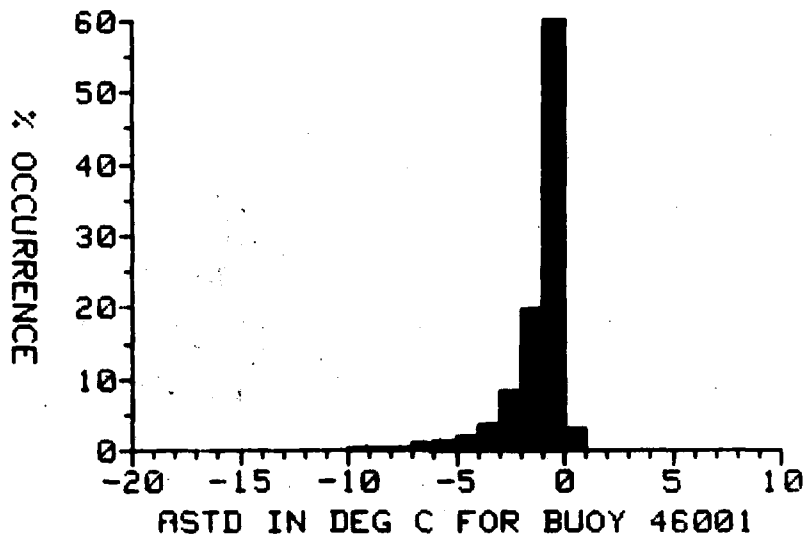
Figure A-16. Annual air-sea temperature difference distribution for buoy 46004 in Marsden square 194.



-16<#	obs<=-14	4	.01%
-14<#	obs<=-12	17	.04%
-12<#	obs<=-10	34	.08%
-10<#	obs<=-8	137	.32%
-8<#	obs<=-6	500	1.17%
-6<#	obs<=-4	1529	3.57%
-4<#	obs<=-2	6307	14.71%
-2<#	obs<= 0	13007	30.34%
0<#	obs<= 2	14100	32.89%
2<#	obs<= 4	5158	12.03%
4<#	obs<= 6	1452	3.39%
6<#	obs<= 8	453	1.06%
8<#	obs<= 10	141	.33%
10<#	obs<= 12	30	.07%
12<#	obs<= 14	4	.01%

Total obs = 42872

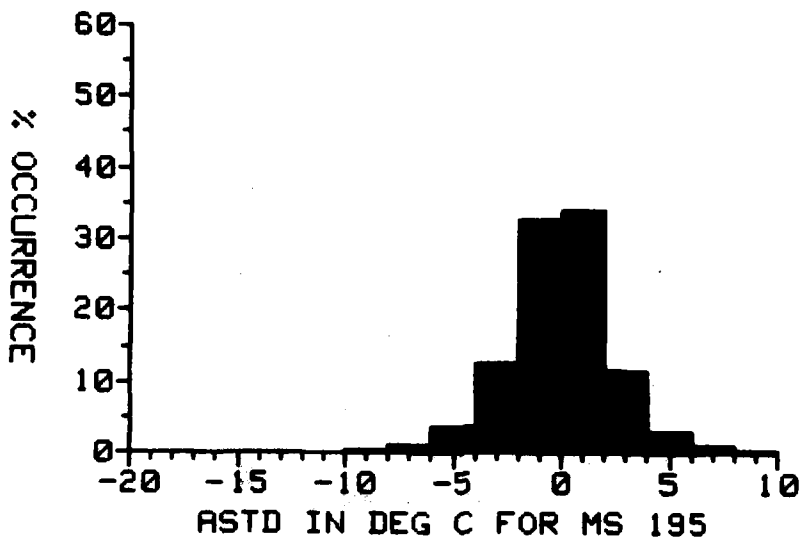
Figure A-17. Annual air-sea temperature difference distribution for Meriden square 194 from IREPS historical data base. Compare with distribution in figure A-16.



-13<# obs<=-12	5	.01%
-12<# obs<=-11	25	.07%
-11<# obs<=-10	36	.10%
-10<# obs<=-9	93	.25%
-9<# obs<=-8	134	.36%
-8<# obs<=-7	145	.39%
-7<# obs<=-6	342	.92%
-6<# obs<=-5	527	1.41%
-5<# obs<=-4	704	1.89%
-4<# obs<=-3	1305	3.50%
-3<# obs<=-2	3111	8.34%
-2<# obs<=-1	7338	19.66%
-1<# obs<= 0	22441	60.13%
0<# obs<= 1	1069	2.86%
1<# obs<= 2	40	.11%
2<# obs<= 3	5	.01%

Total obs = 37320

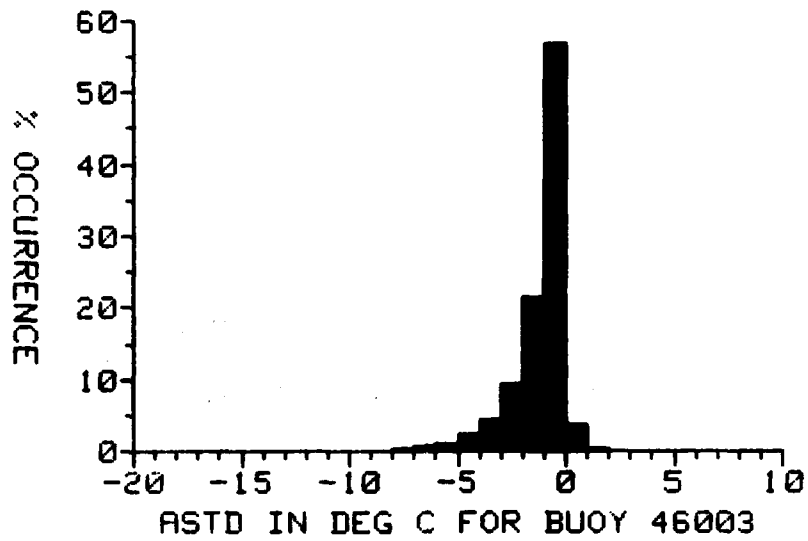
Figure A-18. Annual air-sea temperature difference distribution for buoy 46001 in Marsden square 195.



-14<#	obs<=-12	6	.01%
-12<#	obs<=-10	30	.05%
-10<#	obs<=-8	175	.29%
-8<#	obs<=-6	617	1.02%
-6<#	obs<=-4	2232	3.69%
-4<#	obs<=-2	7633	12.62%
-2<#	obs<= 0	19827	32.78%
0<#	obs<= 2	20553	33.98%
2<#	obs<= 4	6883	11.38%
4<#	obs<= 6	1821	3.01%
6<#	obs<= 8	544	.90%
8<#	obs<= 10	133	.22%
10<#	obs<= 12	24	.04%
12<#	obs<= 14	6	.01%

Total obs = 60486

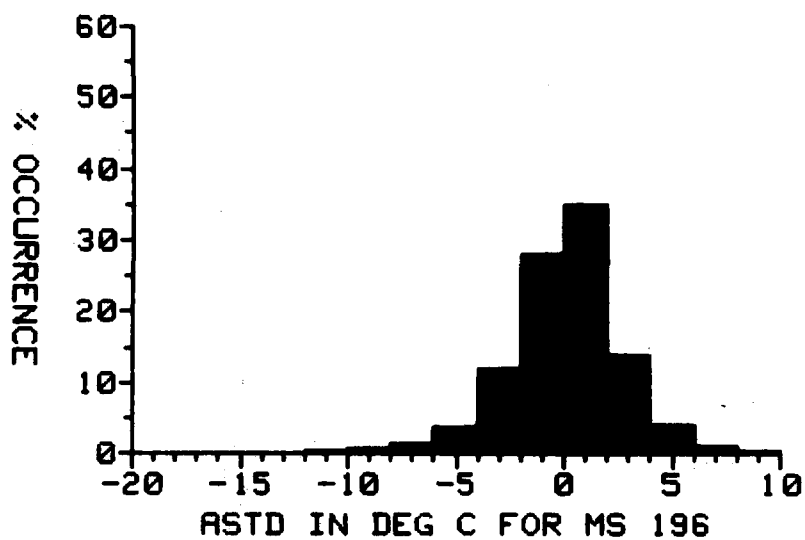
Figure A-19. Annual air-sea temperature difference distribution for Marsden square 195 from IREPS historical data base. Compare with distribution in figure A-18.



-11<# obs<=-10	7	.03%
-10<# obs<= -9	21	.08%
-9<# obs<= -8	48	.14%
-8<# obs<= -7	104	.38%
-7<# obs<= -6	173	.63%
-6<# obs<= -5	291	1.05%
-5<# obs<= -4	593	2.14%
-4<# obs<= -3	1165	4.21%
-3<# obs<= -2	2598	9.39%
-2<# obs<= -1	5972	21.58%
-1<# obs<= 0	15689	56.78%
0<# obs<= 1	962	3.48%
1<# obs<= 2	52	.19%
2<# obs<= 3	2	.01%

Total obs = 27669

Figure A-20. Annual air-sea temperature difference distribution for buoy 46003 in Marsden square 196.



-18<#	obs<=-16	4	.01%
-16<#	obs<=-14	11	.03%
-14<#	obs<=-12	19	.05%
-12<#	obs<=-10	67	.18%
-10<#	obs<= -8	217	.58%
-8<#	obs<= -6	527	1.41%
-6<#	obs<= -4	1374	3.68%
-4<#	obs<= -2	4474	11.97%
-2<#	obs<= 0	10454	27.96%
0<#	obs<= 2	13016	34.81%
2<#	obs<= 4	5173	13.83%
4<#	obs<= 6	1494	4.00%
6<#	obs<= 8	407	1.09%
8<#	obs<= 10	105	.28%
10<#	obs<= 12	37	.10%
12<#	obs<= 14	11	.03%

Total obs = 37389

Figure A-21. Annual air-sea temperature difference distribution for Meraden square 196 from IREPS historical data base. Compare with distribution in figure A-20.

END

FILMED

11-84

DTIC